2014

DEVELOPING A TEST FOR RANDOM NUMBER GENERATORS USING A SIMULATION OF THE HIERARCHICAL POTTS DIAMOND MODEL AT THE CRITICAL POINT

Joshua W. Liberty
University of Rhode Island, shadowofliberty@aol.com

DEVELOPING A TEST FOR RANDOM NUMBER GENERATORS USING A SIMULATION OF THE HIERARCHICAL POTTS DIAMOND MODEL AT THE CRITICAL POINT

BY

JOSHUA W. LIBERTY

A DISSERTATION SUBMITTED IN PARTIAL FULFILLMENT OF THE REQUIREMENTS FOR THE DEGREE OF

DOCTOR OF PHILOSOPHY

IN

PHYSICS

UNIVERSITY OF RHODE ISLAND

2014

DOCTOR OF PHILOSOPHY DISSERTATION

OF

JOSHUA W. LIBERTY

APPROVED:

Dissertation Committee:

Major Professor Peter Nightingale

David Freeman

Leonard M. Kahn

Nasser H. Zawia
DEAN OF THE GRADUATE SCHOOL

UNIVERSITY OF RHODE ISLAND

2014

ABSTRACT

This dissertation uses the hierarchical q-state Potts model at the critical point to develop a new random number generator test. We start with an exposition of renormalization group approach by means of which one can numerically exactly compute the free energy, specific heat and susceptibility of large, but finite lattices. We then show that generalization of these standard techniques allows one to also compute probability distributions related to the energy and the order parameter.

The various computed quantities can be compared with Monte Carlo estimates of the same quantities. We demonstrate that the structure of the hierarchical lattices used allows one to perform the Monte Carlo calculations by direct sampling. This avoids the usual critical slowing down that plagues Monte Carlo calculations at the critical point.

As is well known, critical behavior is highly susceptible to perturbations. We expect that flaws of the pseudo random number generator, such as correlations, will cause statistically significant discrepancies between the results of the simulations and the numerically exactly computed results. Details of the computer code generated for these tests are included.

ACKNOWLEDGMENTS

I would like to thank my mom for her patience with my stress levels as they inevitably varied during the course of this work. Mom, you always had faith in my ability and I appreciate everything you have done for me. I want to thank my father for his inspiring talks of reassurance that my path was always the right one and his belief that I could make it. Thanks to my brother, who, despite his rather sarcastic nature, kept me strong and focused on the task at hand. Thanks to my sister who offered her time to listen to any complaints I had and remained supportive through all my years in academics. I also want to thank Joyce, who never let my times of depression get the best of me, and would bend over backwards just to make me smile.

I want to give a special thanks to my advisor, Dr. Peter Nightingale, who gave me an opportunity to contribute to this beautiful field of science. Dr. Nightingale, you gave me a shot and never gave up on me even when times looked grey. You are a large part of my success and my gratitude for your place in my life goes beyond any words that could be printed on this page, thank you. Finally, thank you to all my friends and family not mentioned above who individually would require more space to thank then is allotted by any institution for this section of my work. All the people in my life have helped make me into who I am today and this work reflects all their hard work in me, thank you all.

DEDICATION

To the Liberty family.

TABLE OF CONTENTS

Page

Page

List of Figures

CHAPTER 1

Introduction

Monte Carlo (MC) methods rely on statistical numerical sampling to obtain results for problems for which deterministic methods fail. Applications of Monte Carlo algorithms include optimization, integration, and making draws from a probability distribution. Results obtained by Monte Carlo methods can be compared with results obtained by numerically exactly calculating thermodynamic properties of statistical mechanical model systems defined on hierarchical lattices. We use this to design a new pseudo random number generator test. We shall henceforth use the acronym RNG in which "pseudo" is implicitly assumed.

In a classical study [1] titled "Monte Carlo simulations: Hidden errors from 'good' random number generators," Ferrenburg demonstrated that random number generators deemed reliable produced systematic errors in Monte Carlo calculations of physical quantities when the generators were used to drive the fast Wolff spin-cluster-flipping algorithm. That the results were biased was determined by comparison with the exact solution to the two-dimensional Ising model by Lars Onsager, which in later work by Ferdinand and Fisher [2] was applied to finite lattices. This dissertation proceeds in the same spirit, and adds some new features to the use of exactly solvable, statistical mechanical models as testing grounds for RNGs.

This dissertation has the following goals:

1. Application of a numerically exact method to a finite hierarchical q-state Potts diamond lattice to obtain thermodynamic properties such as specific heat and susceptibility as well as various probability distributions;

2. Design a direct sampling Monte Carlo method that produces statistical estimates of these quantities;

3. Combine the two approaches to verify the validity of calculated estimators of expectation values and histograms of probability distributions by comparison with dedecoration results. These comparisons are used to verify how well a random number generator performs.

We expect that the sensitivity to correlations of critical systems makes the proposed method a good tool for RNG testing and a useful addition to the standard test suites that are used for this purpose [3], [4].

1.1 The Layout of the Dissertation

Chapter 2 reviews the application of dedecoration to two specific lattice types. These two lattices are the linear periodic chain lattice and the hierarchical diamond lattice. It is shown that thermodynamic quantities such as the free energy are constructed as series expressions that can be obtained by means of recursion in finite lattices or approximated to a desired degree of accuracy in infinite lattices. In the thermodynamic limit, the process of dedecoration makes contact with renomalization group theory. The critical exponents can in principle be obtained by scale invariance used with the models discussed. This shows why various quantities diverge in the thermodynamic limit, but for our tests only finite quantities computed for finite lattices are used.

Chapter 3 discusses the Ising model as a linear chain lattice and as a hierarchical diamond lattice. Linear chains are used as warm-up exercises and to verify segments of our proposed code but they are not of interest in the actual RNG tests. We formulate the computational method of Chapter 2 using a transfer matrix approach. The transfer matrix formulation is convenient and using it allows

us to construct the free energy and heat capacity recursively using dedecoration in both presence and absence of a magnetic field. Finally, the probability distributions of the energy and magnetization are obtained by Fourier transformation of a system with complex interaction parameters. The recursive method solves the problem of exponentially increasing time complexity of brute force summation over the microscopic variables of the lattice.

Chapter 4 generalizes Ising, or two-state, hierarchical diamond lattices to q-state hierarchical diamond Potts lattices. The techniques of Chapter 2 are applied to hierarchical q-state diamond lattices once again using a transfer matrix formulation. The method we use allows us to generalize the model to continuous q. That this can be done is well known, but our approach differs from the standard method; see Ref. [5] and references therein.

Chapter 5 discusses the design of an algorithm that uses Monte Carlo direct sampling to simulate finite hierarchical q-state Potts diamond lattices at the critical point. For thermodynamic quantities we use standard methods to establish possible discrepancies between recursively computed quantities and the results obtained by Monte Carlo. To determine if probability distributions agree with theoretical predictions we collect the number of times a particular value of energy or magnetization is realized in histogram bins. The observed frequencies and the corresponding probabilities can be compared with theoretical prediction by means of the χ^2 statistic. For the latter to be applicable we have to take into account that certain bins of the histograms will be sparsely populated. As a consequence, their contents after a Monte Carlo run of a certain length will be not be even approximately normally distributed. This problem can be solved by combining bins into sufficiently large super-bins, i.e., by *coarse-graining*. We conclude by a discussion of what remains to be done in subsequent research.

List of References

[1] D. L. A.M. Ferrenburg and Y. Wong, "Monte Carlo simulations: Hidden errors from 'good' random number generators," *Physical Review*, vol. 69, 3382, 1992.

[2] A. Ferdinand and M. Fisher, "Bounded and Inhomogenous Ising Models. I. Specific-Heat Anomaly of a Finite Lattice," *Physical Review*, vol. 185, 932, 1969.

[3] Wikipedia. "Diehard tests." aug 2011. [Online]. Available: http://en.wikipedia.org/wiki/Diehard_tests

[4] TestU01. "Testu01." aug 2009. [Online]. Available: http://www.iro.umontreal.ca/~simardr/testu01/tu01.html

[5] F. Wu, "The Potts model," *Reviews of Moden Physics*, vol. 54 No. 1, jan 1982.

CHAPTER 2

Review of Renormalization Group Theory

This dissertation restricts itself to two types of lattices; the linear chain lattice and the hierarchical diamond lattice. Both will be specified by notation L_l where $l = 1, 2, ...$ denotes the recursion level of lattice L. In the chain lattice configuration L_1 denotes a system with two sites connected by two bonds. The lattices L_{l+1} of the chain are recursively constructed by placing a new site between existing sites; see Figures 1, 2, 3. In the hierarchical lattice, L_1 defines a system of two sites connected by one bond. Hierarchical lattices L_{l+1} are recursively constructed by replacing this unit by a diamond, as illustrated Figures 4, 5, 6.

We define n_l^s and n_l^b as the number of sites and bonds of lattice L_l. The relationship of sites and bonds for both lattices based on level l are determined by recursion relations. In the chain lattice,

$$n_l^s = n_l^b = 2^l. \tag{1}$$

Note, in the chain lattice, $n_l^s = n_l^b$, which corresponds to a chain with periodic boundary conditions. In the hierarchical lattice,

$$n_l^s = (4^l + 8)/6, \tag{2}$$

$$n_l^b = 4^{l-1}. \tag{3}$$

The microscopic variables located on the sites of the lattice L_l are denoted in general by configurations $S_l = (s_1, s_2, \ldots, s_{n_l^s})$. The site variables take on discrete values called states: ± 1 for the Ising model and $1, \ldots, q$ for the q-state Potts model. The process of adding a site between two existing ones is called decoration.

The construction of the diamond lattice requires bond doubling combined with decoration.

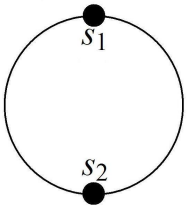

Figure 1. Chain lattice L_1

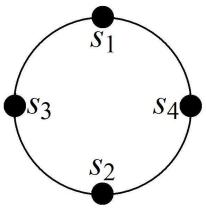

Figure 2. Chain lattice L_2

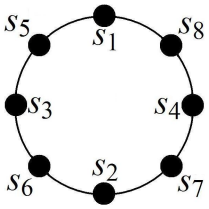

Figure 3. Chain lattice L_3

Figure 4. Hierarchical lattice L_1

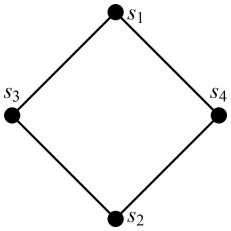

Figure 5. Hierarchical lattice L_2

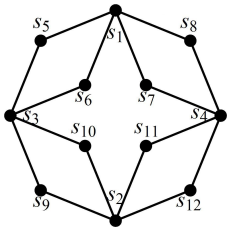

Figure 6. Hierarchical lattice L_3

2.1 Recursion by Dedecoration

We associate with each pair of sites (s_i, s_j) the energy $\epsilon(s_i, s_j; K)$. K is the set of all interaction parameters, which will be specified in the following chapters. We also adopt the convention that defines the zero of the energy and absorb the Boltzmann factor, $-1/k_{\mathrm{B}}T$, into the energy. This reduced energy will simply be called the energy. We introduce a transfer matrix corresponding to the fact that we consider the energy of the system to be a sum of only single-site and nearest-neighbor contributions:

$$T(s_i, s_j; K) = \exp[\epsilon(s_i, s_j, K)]. \tag{4}$$

Dedecoration is the process of summing over all sites with two nearest neighbors in lattice L_l. In the linear configuration, since connectivity does not vary, this process is nothing but summing over the microscopic variable at every other site in the chain. Here, and in following chapters, we deal mostly with finite systems; we will only consider the thermodynamic limit for theoretical purposes when needed.

The first lattice we discuss is the linear chain. The process of dedecoration is illustrated in Figure 7. In terms of matrix multiplication, dedecoration takes the following form:

$$\sum_{s_3} T(s_1, s_3; K)T(s_3, s_2; K) = gT(s_1, s_2; K'). \tag{5}$$

We see that dedecoration in this system reduces the lattice from three to two sites and introduces a changed interaction parameter $K \to K'(K)$ along with a shifted term $g = g(K)$ to reimpose the zero energy convention used. Note, the set of parameters K must be sufficiently general enough to make sure that no new ones are generated in the process of dedecoration. For the Ising chain, nearest neighbor coupling satisfies this requirement both in the presence and absence of a magnetic field. The case of the q-state Potts model is more complicated as we shall see in Chapter 4.

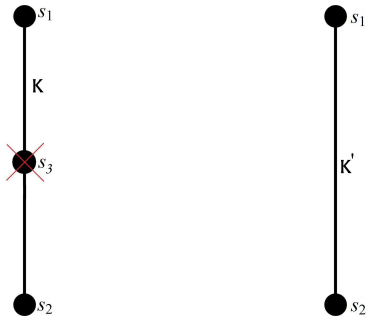

Figure 7. Dedecoration for the linear chain.

The essential transformation required to generate the recursion relations of the hierarchical lattice is illustrated in Figure 8. All that needs to be added,

compared to the case of the linear chain, is the bond doubling:

$$\left(\sum_{s_3} T(s_1, s_3; K)T(s_3, s_2; K)\right)\left(\sum_{s_4} T(s_1, s_4; K)T(s_4, s_2; K)\right) = g'T(s_1, s_2; K''). \tag{6}$$

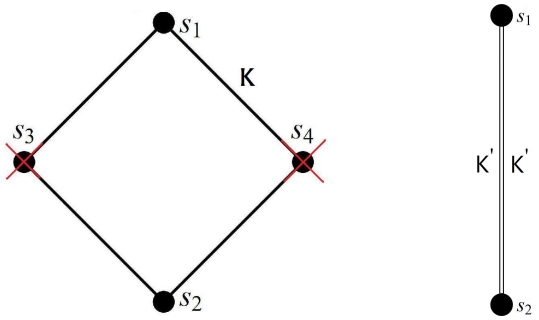

Figure 8. The dedecoration and bond doubling for the hierarchical lattice.

In operations like Eq. (6) one can immediately see the relationship to single site dedecoration, $g'(K) = g(K)^2$ and $K''(K) = 2K'(K)$. The change in interactions is visually shown in Figure 8 where summing over s_3 and s_4 reduces the hierarchical L_2 lattice to the hierarchical L_1 lattice with two modified parameters of interaction K'. For the rest of this chapter we consider hierarchical lattices only; the modifications between the two lattices are straightforward and this will allow the notation to remain simple.

The general Hamiltonian that describes all systems specified by configuration S_l and the set of all interaction parameters, K, is written as $\mathcal{H}(S_l, K)$. We remind the reader that $-1/k_{\mathrm{B}}T$ has been absorbed into the energy. In terms of the transfer matrix of Eq. (4), the Boltzmann weight of a configuration of a lattice of level l is given by

$$\prod_{\langle i,j\rangle \in L_l} T(s_i, s_j; K) = \exp[\mathcal{H}_l(S_l, K)], \tag{7}$$

where $\langle i, j\rangle \in L_l$ denote all nearest neighbor pairs in L_l. We now define the

partition function of lattice level l using Eq. (7),

$$Z_l(K) = \sum_{S_l} \left(\prod_{\langle i,j \rangle \in L_l} T(s_i, s_j; K) \right) = \sum_{S_l} \exp[\mathcal{H}_l(S_l, K)]. \tag{8}$$

Consider the hierarchical lattice L_3 and apply dedecoration once. To accomplish this transformation from L_3 to L_2 in Figures 5 and 6 we open up $\sum_{S_l}$ and act out all sums on sites $s_5, s_6, \ldots, s_{12}$ with operations like Eq. (6). After dedecoration, the remaining sums act on the lowered lattice of modified interactions. Therefore, dedecoration relates a starting partition function of level l to partition function of level $l-1$ with modified interaction parameters,

$$Z_l(K) = G_{l-1}(K) Z_{l-1}(K'). \tag{9}$$

The factor $G_{l-1}(K)$ is a by-product of normalizing the shift in energy that comes from operations Eq. (6). Each bond after dedecoration contributes to the overall shift in energy and so $G_{l-1}(K)$ has a power of bond contributions of the dedecorated lattice, $G_{l-1}(K) = (g'(K))^{n_{l-1}^b}$. Using dedecoration, we generate a recursive method of evaluating the partition function. Note, dedecoration can be repeatedly applied until our system reaches the point at which one chooses to calculate the partition function by explicit summation.

2.1.1 The Free Energy and Renormalization

Taking the logarithm of the recursion relation for the partition function in Eq. (9) gives a recursive relationship of the reduced free energy

$$F_l(K) = \log Z_l(K) = \log G_{l-1}(K) + \log Z_{l-1}(K') = n_{l-1}^b \log g'(K) + F_{l-1}(K'). \tag{10}$$

Dividing Eq. (10) by the number of bonds, n_l^b, gives the recursion relationship of the free energy per bond,

$$f_l(K) = \frac{n_{l-1}^b}{n_l^b} \log g'(K) + \frac{n_{l-1}^b}{n_l^b} f_{l-1}(K'), \tag{11}$$

where $f_l(K) = F_l(K)/n_l^b$, and $f_{l-1}(K') = F_{l-1}(K')/n_{l-1}^b$. The recursive form of the free energy can be used to compute numerically exact results for finite lattices and approximations correct to any desired accuracy for infinite models; see Chapters 3, 4 for applications.

In the thermodynamic limit Eq. (11) shows that the hierarchical model is self-similar if the first term on the right is interpreted as self-energy associated with each site. We write f for the free energy per site in the thermodynamic limit and define $g''(K) = \lim_{l\to\infty} \frac{n_{l-1}^b}{n_l^b} \log g'(K)$. To make contact with the usual scaling relation for the free energy [1] we have written $\lim_{l\to\infty} \frac{n_{l-1}^b}{n_l^b} = 4 = b^d$ where $b = 2$ is the rescaling length and $d = 2$ can be thought of as the dimensionality of the system. The free energy per bond in the thermodynamic limit satisfies the well-known scaling relation

$$f(K) = g(K) + b^{-d} f(K'). \tag{12}$$

In Eq. (12) all double primes have been dropped; we settle on a unique notation of g, K' for the remainder of the chapter.

Renormalization group (RG) theory was developed to obtain critical point exponents describing critical point singularities and explain the observed universality of critical behavior [2] of the free energy per bond $f(K)$ from the regular functions $g(K)$ and $K'(K)$. In general there is no guarantee that $g(K)$ and $K'(K)$ are regular at the critical point. However, in the case of the hierarchical lattices we consider, this property is rigorously satisfied by the summation over sites with only two nearest neighbors at every level of dedecoration; the dedecoration operation is a modified RG transformation. It is well-known that the scaling transformation implies that the free energy has power-law singularities that are characterized by critical exponents. We therefore continue to review the standard approach.

The renormalization group equations are

$$K' = K'(K). \tag{13}$$

Fixed points are points in parameter space that are invariant under the RG transformation:

$$K'(K^*) = K^*. \tag{14}$$

There typically are several fixed points for any transformation, but some, such as zero and infinite temperature fixed points, are only indirectly relevant for critical behavior. We are interested in non-trivial fixed points for our analysis. The linearized form of the transformation of interaction to interaction $K' = K'(K)$ is determined by the Jacobian matrix

$$\frac{\partial K'_\alpha}{\partial K_\beta} = T_{\alpha\beta}. \tag{15}$$

Here, α, β are matrix indexes of the Jacobian. The fixed point of the linearized transformation is

$$\left(\frac{\partial K'_\alpha}{\partial K_\beta}\right)_{K^*} = T^*_{\alpha\beta}. \tag{16}$$

With the Jacobian, the linearized transformation reads

$$K'_\alpha - K^*_\alpha = \sum_\beta T^*_{\alpha\beta}(K_\beta - K^*_\beta). \tag{17}$$

To simplify the transformation in Eq. (17) one can introduce normal mode coordinates. Consider $T^*_{\alpha\beta}$ to have eigenvalues λ_i with left eigenvectors ϕ^i_α such that

$$\sum_\alpha \phi^i_\alpha T^*_{\alpha\beta} = \lambda_i \phi^i_\beta. \tag{18}$$

Thus, we obtain

$$u_i = \sum_\alpha \phi^i_\alpha (K_\alpha - K^*_\alpha). \tag{19}$$

In normal-mode coordinates the RG transformation takes the form

$$u_i' = \sum_\alpha \phi_\alpha^i (K_\alpha' - K_\alpha^*) = \lambda_i \sum_\beta \phi_\beta^i (K_\beta - K_\beta^*) = \lambda_i u_i. \tag{20}$$

The interaction parameters are expressed in terms of the scaling coordinates (or scaling fields) since the coordinates are functions of the interaction parameters, $\lambda_i u_i(K) = u_i(K')$. Note that $\lambda = 1$ will change nothing; this value of λ is neither a relevant or irrelevant change. $\lambda = 1$ is the marginal value and it sets the bounds for the two cases $\lambda > 1$ (relevant) and $\lambda < 1$ (irrelevant). We write

$$\lambda_i = b^{y_i}, \tag{21}$$

and we shall treat b as a continuous variable. The justification for this is that the RG transformation can be iterated, but this approach obscures some subtleties that are of no interest here. We refer to to the literature for details [2].

2.2 Scaling Theory

We next review the implications of the scaling equation for the free energy

$$f(u_1, u_2, ...) = g(u_1, u_2, ...) + b^{-d} f(b^{y_1} u_1, b^{y_2} u_2, ...). \tag{22}$$

We restrict ourselves to the case of two scaling fields, u_1, a thermal field and u_2 a field coupling to the order parameter.

2.2.1 The Regular and Singular Free Energy

We consider two parts to the free energy: the regular part and the singular part. To keep things simple we look at the case of a single, thermal scaling field, only,

$$f(u) = f_{\text{reg}} + f_{\text{sing}}. \tag{23}$$

As discussed above $g = g(u)$ is a regular function even at the critical point. If the regular part of the free energy satisfies

$$f(u)_{\text{reg}} = g(u) + b^{-d} f(u')_{\text{reg}}, \tag{24}$$

we find that the singular part satisfies the homogeneous equation

$$f(u)_{\text{sing}} = b^{-d} f(u')_{\text{sing}}. \tag{25}$$

For details, see the work of Niemeijer and van Leeuwen [2].

2.2.2 Widom Scaling

Eq. (23) was obtained for one scaling parameter, but its form generalizes for multiple scaling parameters; see Section 2.2. The singular part that satisfies the well-known Widom homogeneity relation, implies scaling relations for critical exponents that describe the divergences of various quantities of the system [1], [3]. We briefly review the main results here. The distance from the critical temperature, T_c, can be defined as

$$\tau = \frac{T - T_c}{T_c}. \tag{26}$$

Near the critical temperature the singular behavior of the specific heat, spontaneous magnetization, magnetic susceptibility, and response to magnetic field at T_c are given by the exponents α, β, γ and δ: $C \simeq |\tau|^{-\alpha}$, $m \simeq (-\tau^{\beta})$, $\chi \simeq |\tau|^{-\gamma}$, and $h = |m|^{\delta}$. The homogeneous singular piece of the free energy for two scaling fields, $u_1 = u_T$, the thermal bonding scaling field, and $u_2 = u_h$ as the external magnetic scaling field gives for Eq. (25),

$$f_{\text{sing}}(b^{y_T} u_T, b^{y_h} u_h) = b^d f_{\text{sing}}(u_T, u_h), \tag{27}$$

where y_T, y_h are parameters that characterize the homogeneous function of degree d. Kadanoff [4] showed that d is the dimensionality of the lattice and in agreement with analysis of the renormalization approach to our models as discussed above.

First we can obtain the critical exponent of the magnetization, β, by differentiating Eq. (27) with respect to u_h,

$$b^{y_H} m(b^{y_T} u_T, b^{y_h} u_h) = b^d m(u_T, u_h). \tag{28}$$

Let $b = (-u_T)^{-1/y_T}$ and $u_h = 0$ so

$$m(u_T, 0) = (-u_T)^{(d-y_h)/y_T} m(-1, 0). \tag{29}$$

The thermal scaling field u_T is proportional to τ which yields

$$\beta = \frac{d - y_h}{y_T}. \tag{30}$$

Next, the degree of the critical isotherm, δ, is obtained by differentiating Eq. (27) with respect to u_h and setting $u_T = 0$ and $b = u_h^{1/y_h}$,

$$m(0, u_h) = (u_h)^{(d-y_h)/y_h} m(0, 1). \tag{31}$$

Noting u_h is proportional to the ordering field h, we find that

$$\delta = \frac{y_h}{d - y_h}. \tag{32}$$

Magnetic susceptibility is found through differentiation of Eq. (27) twice with respect to u_h,

$$b^{2y_h} \chi(b^{y_T} u_T, b^{y_h} u_h) = b^d \chi(u_T, u_h). \tag{33}$$

Setting $u_h = 0$ and letting $b = (u_T)^{-1/y_T} = (\tau)^{-1/y_T}$,

$$\chi(\tau, 0) = \tau^{(d-2y_h)/y_T} \chi(1, 0). \tag{34}$$

Hence, the critical exponent for susceptibility reads

$$\gamma = \frac{2y_h - d}{y_T}. \tag{35}$$

Finally, the critical exponent of the specific heat at constant field is given by differentiation of Eq. (27) twice with respect to u_T,

$$b^{2y_T} C(b^{y_T} u_T, b^{y_h} u_h) = b^d C(u_T, u_h). \tag{36}$$

Again, setting $u_h = 0$ and $b = (u_T)^{-1/y_T} = (\tau)^{-1/y_T}$ gives

$$C(\tau, 0) = \tau^{(d-2y_T)/y_T} C(1, 0), \tag{37}$$

and, we conclude that

$$\alpha = 2 - \frac{d}{y_T}. \tag{38}$$

The four critical exponents are obtained through the scaling parameters y_T, y_h. Combining the expressions for the critical exponents yields relationships between the four. Consider the combination of Eqs. (30), (32), and (35) which give

$$\gamma = \beta(\delta - 1). \tag{39}$$

From Eqs. (30), (32), and (38) we find

$$\alpha + \beta(\delta + 1) = 2. \tag{40}$$

Hence, we obtain exact relationships for the critical exponents using scaling theory.

An identification used in getting the critical exponents came from operations like $b = (u_T)^{-1/y_T} = (\tau)^{-1/y_T}$ (specific heat). This choice of b is related to the fact that at critical points the correlation length of the system becomes infinite; the fluctuations in the system become correlated over all distances. In other words, the correlation length is observed to go as $(\tau)^{-1/y_T}$ so we choose b on the order of the same length as the correlation length. We can think of repeatedly applying renormalization transformations to an infinite system in the neighborhood of a critical point until the correlation length is of order unity.

2.2.3 Finite-Size Scaling

We can also obtain finite-size scaling relations [5]. We consider the inverse system size itself as a scaling field. This analysis yields the specific heat and susceptibility as a function of system size. Consider Eq. (27), but with a third

scaling field, $u_3 = 1/a$, with a as the total linear system size measured in lattice units. If the system is scaled by b the inverse system size transforms as $a^{-1} \to ba^{-1}$,

$$f_{\text{sing}}(b^{y_T}u_T, b^{y_h}u_h, b/a) = b^d f_{\text{sing}}(u_T, u_h, 1/a). \tag{41}$$

Similar to the behavior of u_T, u_h at the critical point, the inverse system size also tends to zero through dedecoration. Following the same procedure of obtaining the specific heat and susceptibility previously will lead to results like Eqs. (33) and (36) with the new scaling field present in the argument of the functions. Choosing $b = (1/a)^{-1}$ yields the following result for each,

$$\chi(\tau, 0, 1/a) = a^{2y_h - d}\chi(a^{y_T}\tau, 0, 1), \tag{42}$$

$$C(\tau, 0, 1/a) = a^{2y_T - d}C(a^{y_T}\tau, 0, 1). \tag{43}$$

The exponents on the right hand side of these equations can be positive or negative corresponding to a divergence in the infinite system limit or approach to a finite limit.

List of References

[1] K. Huang, *Statistical Mehcanics, 2nd. edn.* Hoboken, New Jersey, United States of America: John Wiley and Sons, INC., 1987.

[2] T. Niemeijer and J. van Leeuwen, *Phase transitions and critical phenomena, Voulme 7, Chapter 7.* Waltham, Massachusetts, United States of America: Academic Press, 1972-2001.

[3] L. E. Reichl, *A Modern Course in Statistical Physics.* Austin, Texas, United States of America: University of Texas Press, 1980.

[4] L. Kadanoff, "Scaling laws for Ising models near critical temperature," *Physics*, vol. 2, 263, 1966.

[5] A. Ferdinand and M. Fisher, "Bounded and Inhomogenous Ising Models. I. Specific-Heat Anomaly of a Finite Lattice," *Physical Review*, vol. 185, 932, 1969.

CHAPTER 3

The Ising Model

The Ising model, named after Ernst Ising, is a nearest-neighbor spin-dependent statistical mechanics model [1]. Although the model is simple, it is believed to correctly describe the critical behavior of systems that have order parameters with the same symmetry properties. The linear chain exhibits some of the characteristics of more sophisticated systems and is presented as a warm-up exercise for constructing the RG equations. After that, we deal with the hierarchical diamond lattice for critical phenomena that is not present in the chain model. The lattice types we use are defined in Chapter 2. In both types of lattices we apply the techniques of dedecoration to obtain the desired statistical quantities that serve to produce the theoretically computed quantities used in the RNG tests we develop.

3.1 Classical Interpretation of the Ising Model

It is well-known that below the critical temperature microscopic spins can align over macroscopic distances in some systems. This is known as long-range order and in these systems it can produce macroscopic spontaneous magnetization. Above the critical temperature the spins display only short-range order which produces no net macroscopic arrangement. The Ising model can be used to help describe this process seen in nature [2], [3], [4], [5]. The Ising model is a discrete spin model; the site state variables can either be +1 or -1 representing spin up and spin down. Here we are mainly interested in the sensitivity of the critical point for small perturbations that might be introduced by correlations in RNGs used in Monte Carlo simulations.

Recall that Hamiltonian of L_l is reduced to dimensionless form by absorbing

$\beta = -1/k_{\mathrm{B}}T$ in the coupling constants κ and h. The reduced energy of a spin configuration S_l is

$$\mathcal{H}_l(S_l, \kappa, h) = \kappa \sum_{\langle ij \rangle \in L_l} s_i s_j + h \sum_{i=1}^{n_l^s} s_i. \tag{44}$$

In this sum $\langle i, j \rangle$ runs over all pairs of nearest-neighbors of the lattice L_l and i runs over the sites. The coupling constant $\kappa = -\beta\epsilon$ determines the nearest-neighbor pair interaction coupling for nearest neighbors and h is the coupling with the external magnetic field. The partition function is given by

$$Z_l(\kappa, h) = \sum_{S_l} e^{\mathcal{H}_l(S_l, \kappa, h)}, \tag{45}$$

where each s_i in S_l assumes the values ± 1. Dedecoration is conveniently described in terms of the the transfer matrix, as defined in Chapter 2. For the Ising model it takes the following explicit form

$$T = \begin{bmatrix} e^{\kappa+h} & e^{-\kappa} \\ e^{-\kappa} & e^{\kappa-h} \end{bmatrix}. \tag{46}$$

3.2 The Linear Ising Chain

In the linear Ising model the system is constructed as a periodic chain of dipoles; see Figures 1, 2, 3. The energy for a configuration S_l is

$$\mathcal{H}_l(S_l, \kappa, h) = \kappa \sum_{i=1}^{n_l^s} s_i s_{i+1} + h \sum_i s_i, \tag{47}$$

with the periodic boundary condition $s_{n_l^s+1} = s_1$. The Hamiltonian in the absence of a field simplifies to pair-coupling energy only and the transfer matrix becomes

$$T_{h=0} = \begin{bmatrix} e^{\kappa} & e^{-\kappa} \\ e^{-\kappa} & e^{\kappa} \end{bmatrix}. \tag{48}$$

Squaring the transfer matrix corresponds to dedecoration, as discussed in the previous chapter; see section 2.1,

$$T_{h=0} \cdot T_{h=0} = \begin{bmatrix} e^{2\kappa} + e^{-2\kappa} & 2 \\ 2 & e^{2\kappa} + e^{-2\kappa} \end{bmatrix} = T'_{h=0}. \tag{49}$$

This matrix can be written as

$$T'_{h_l=0} = g(\kappa) \begin{bmatrix} e^{\kappa'(\kappa)} & e^{-\kappa'(\kappa)} \\ e^{-\kappa'(\kappa)} & e^{\kappa'(\kappa)} \end{bmatrix}, \tag{50}$$

with g and κ' determined by

$$e^{2\kappa} + e^{-2\kappa} = g(\kappa) e^{\kappa'(\kappa)}, \tag{51}$$

$$2 = g(\kappa) e^{-\kappa'(\kappa)}. \tag{52}$$

Solving Eqs. (51) and (52) gives

$$g(\kappa) = 2\sqrt{\cosh 2\kappa}, \tag{53}$$

$$\kappa'(\kappa) = \frac{1}{2} \log \cosh 2\kappa. \tag{54}$$

The factor g introduced in Eq. (50) follows from the zero of energy convention implicit in the definition of the Hamiltonian.

If L_l starts with κ everywhere then one operation of dedecoration, in terms of how coupling pair interactions change under subsequent steps of the dedecoration transformation, can be defined as

$$\kappa_1(\kappa) = \kappa'(\kappa). \tag{55}$$

Repeated applications of dedecoration continue to apply the same type of interaction transformations. Successive transformations can be obtained by recursion,

$$\kappa_k(\kappa) = \kappa_1[\kappa_{k-1}(\kappa)]. \tag{56}$$

Here, k is a positive integer that denotes the number of times the interactions transformed, *i.e.,* a second dedecoration operation would give $\kappa_2 = \kappa_1[\kappa_1(\kappa)] = \kappa_1 \circ \kappa_1(\kappa)$. In the subscript notation applied to pair interactions it is understood that $\kappa_0 = \kappa$.

One application of dedecoration performs a summation over half of the sites. The g term to the power of remaining bonds of the dedecorated lattice gives the overall energy shift, G, and the partition function according to Eqs. (53) and (54) can be constructed as

$$Z_l(\kappa) = G_{l-1}(\kappa) Z_{l-1}(\kappa_1) = g(\kappa)^{n_{l-1}^b} Z_{l-1}(\kappa_1). \tag{57}$$

To calculate the partition function by recursion from starting lattice L_l we repeatedly square the transfer matrix. Any finite chain can be reduced by a finite number of dedecoration transformations to a system small enough to calculate the partition function directly. If the chain was infinitely sized, then the process described in this section could be applied repeatedly until a quantity such as the free energy per site has converged to a desired accuracy. A property of the zero-field linear Ising chain is that

$$\kappa_k > \kappa_{k+1}. \tag{58}$$

This property of the function κ' shows that there is no phase transitions in the linear system. The only fixed points in this system are the infinite and zero temperature limit.

3.2.1 Linear Ising Lattice Free Energy, Total Energy, and Heat Capacity

As mentioned before, we use the term free energy as short for the reduced free energy, *i.e.,* the free energy multiplied by $-1/k_{\mathrm{B}}T$; see Section 2.1.1. The total energy and heat capacity that follow from our definition of the free energy are therefore not given by their usual expressions and are also in reduced form. Using the reduced forms of these quantities does not alter the results presented in this dissertation other than by scaling in various powers of temperature, which is of no significance for our purpose.

The first derivative of free energy in the linear chain configuration for level l with respect to κ and no external field gives the total energy U as

$$U_l(\kappa) = n_{l-1}^b \frac{\partial}{\partial \kappa} \log g(\kappa) + \frac{\partial \kappa_1}{\partial \kappa} U_{l-1}(\kappa_1). \tag{59}$$

We consider four systems, $n_l^b = 4$, 8, 16, and 32 bonds, representing L_2, L_3, L_4, and L_5; the results of the energy are plotted in Figure 9. Another derivative with respect to κ gives the heat capacity of the system, C, which in the reduced quantities we use is nothing but the variance of the reduced energy, see Figure 10,

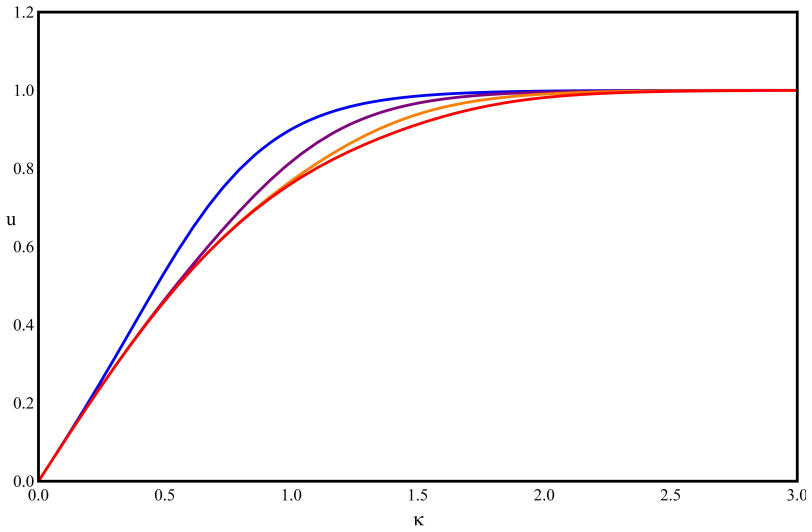

Figure 9. The coupling energy for the linear Ising system per bond. We have four systems of varying size, $n_l^b = 4$ (blue), 8 (purple), 16 (orange), and 32 bonds (red).

$$C_l(\kappa) = n_{l-1}^b \frac{\partial^2}{\partial \kappa^2} \log g(\kappa) + \frac{\partial^2 \kappa_1}{\partial \kappa^2} U_{l-1}(\kappa_1) + \left(\frac{\partial \kappa_1}{\partial \kappa} \right)^2 C_{l-1}(\kappa_1). \tag{60}$$

Notice, the energy and heat capacity are constructed as a series that can be solved recursively. Dedecoration provides a method to compute numerical exact values of desirable statistical quantities in the Ising chain in finite models or until a desired point of precision in infinite models.

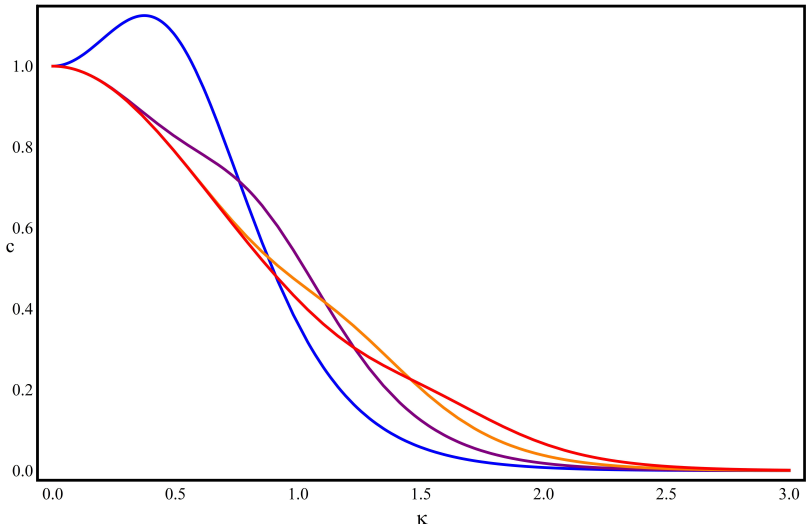

Figure 10. The heat capacity per bond for the linear Ising system. We have four systems of varying size, $n_l^b = 4$ (blue), 8 (purple), 16 (orange), and 32 bonds (red).

3.3 The Hierarchical Ising Diamond

Here we consider the hierarchical diamond lattices in Figures 4, 5, and 6. The Hamiltonian with bond interaction κ and field interaction h is given in Section 3.1; see Eq. (44). The transfer matrix method is applied as explained in Section 2.1, Eq. (6).

3.3.1 The Hierarchal Ising Lattice Phase Transition

In the absence of an external field Eq. (44) reduces to

$$\mathcal{H}_l(S_l, \kappa) = \kappa \sum_{\langle i,j\rangle \in L_l} s_i s_j. \tag{61}$$

Pair-site dedecoration for level l results in bond doubling in this case; see Figure 8. The transfer matrix for the hierarchical Ising diamond lattice is still Eq. (48) and factorizes to a form like Eq. (50). To account for bond-doubling both transfer matrix results from the linear Ising lattice are squared in the analysis of dedecoration applied to hierarchical lattices,

$$g'(\kappa) = g(\kappa)^2 = \left(2\sqrt{\cosh 2\kappa}\right)^2, \tag{62}$$

$$\kappa''(\kappa) = 2\kappa'(\kappa) = \log[\cosh 2\kappa]. \tag{63}$$

Following Section 3.2 for how interactions change under subsequent steps of the dedecoration transformation, we similarly write how interactions change in the hierarchical diamond lattice as

$$\kappa_1(\kappa) = \kappa''(\kappa). \tag{64}$$

The function κ'' exhibits new properties that were not present in the linear example. If $\kappa_1 = \kappa$ there is a critical fixed point and if at this critical point the interactions repeatedly transform into the same interactions. The interaction at the fixed point is denoted as the critical coupling pair interaction κ_c and its numerical value is given as

$$\kappa_c = 0.609378. \tag{65}$$

Starting dedecoration above or below the critical point will tend the interactions towards the trivial fixed points at zero or infinite temperature. The problem has three fixed points in total now, two are trivial, and the third, κ_c, is the desired fixed point associated with the phase transition.

3.3.2 Hierarchical Diamond Lattice Total Energy and Heat Capacity

The total energy and heat capacity of the hierarchical Ising diamond lattices are constructed by means of two coupled recursion relations

$$U_l(\kappa) = n_{l-1}^b \frac{\partial}{\partial \kappa} \log g'(\kappa) + \frac{\partial \kappa_1}{\partial \kappa} U_{l-1}(\kappa_1), \tag{66}$$

$$C_l(\kappa) = n_{l-1}^b \frac{\partial^2}{\partial \kappa^2} \log g'(\kappa) + \frac{\partial^2 \kappa_1}{\partial \kappa^2} U_{l-1}(\kappa_1) + \left(\frac{\partial \kappa_1}{\partial \kappa}\right)^2 C_{l-1}(\kappa_1). \tag{67}$$

In Figure 11 the energy and heat capacity per bond of the hierarchal Ising diamond lattice for various system sizes are shown. Notice that the specific heat has a rounded cusp at κ_c that becomes sharper as system size increases. The linear

chain which lacks a phase transition does not have this feature and is expected to be less sensitive to flaws in the RNGs that we want to test by means of Monte Carlo simulation. Compare with Figure 10. Of course, in the hierarchical lattice, only the infinite Ising system has a true cusp.

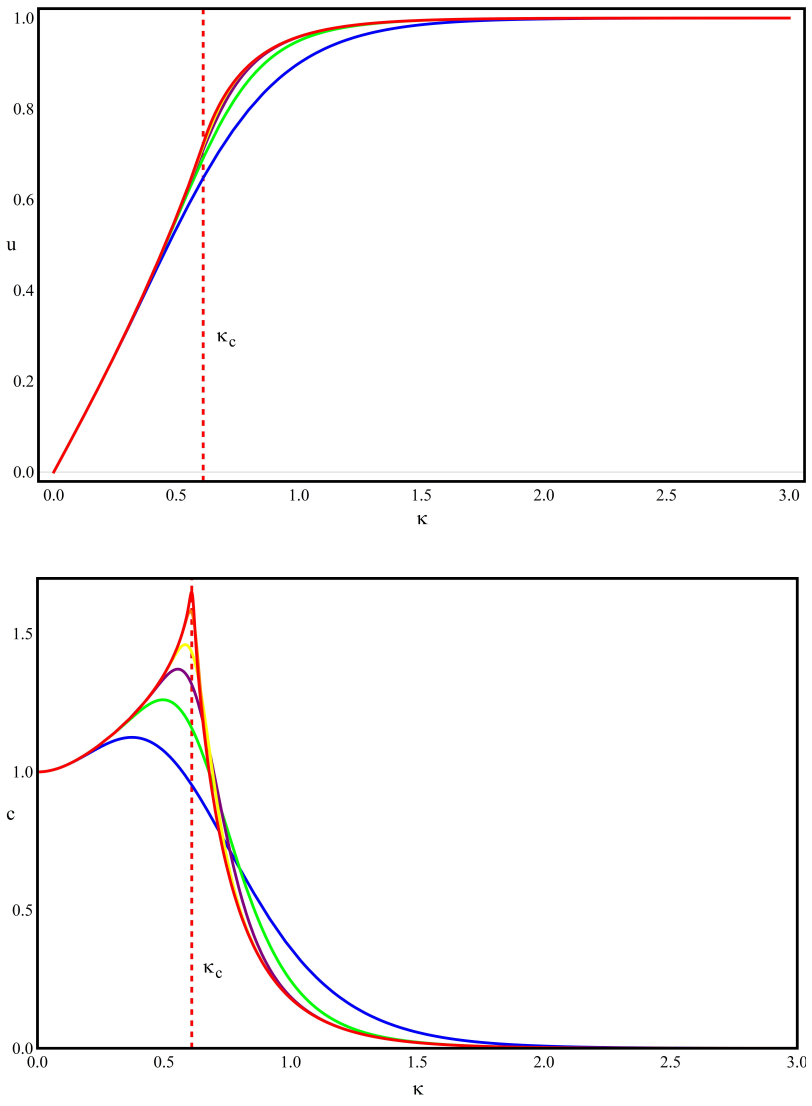

Figure 11. The energy (pair-coupling) and heat capacity graphs per bond for hierarchal systems L_2, L_3, L_4, L_5, L_7, and L_9 with κ_c included. Notice as systems increase in size divergent phenomena appears about the critical point.

3.3.3 The Analysis of the Hierarchal Lattice System with Field

The previous sections excluded an external field in the system. When the interaction K was just pair-coupling κ in the hierarchical models then dedecoration of L_l to L_{l-1} would produce bond-doubling between all neighbors. To correctly account for bond-doubling in computing the partition function of the L_{l-1} hierarchical model, the general expressions for the shift of energy, g, and renormalized pair-coupling, κ', both needed to be squared; see Section 3.3.1. Upon dedecoration in systems with an external field, sites with a field will be summed over; these fields must be conserved and so they will be renormalized, split, and propagate to neighboring sites. The remaining sites with their fields will get contributions of the propagated fields depending on how many neighbors the remaining site originally had. This implies that if one starts with a system with uniform interactions that a single recursion step will destroy this property; this is something that does not happen in the absence of a magnetic field. Repeated recursion generates a hierarchy of coupling constants, as will be shown in detail below.

We begin by defining the general results of dedecoration in the presence of an external field; these results are the energy shift $g(\kappa, h)$, the renormalized bonding $\kappa'(\kappa, h)$, and the renormalized field $h'(\kappa, h)$. Until this point we have never considered a site interaction term in K using dedecoration and have only dealt with pair-coupling transformations and the shifts in energy that follow. Therefore, we step back from hierarchical models and look at a variation of our linear Ising chains. Consider an isolated three site system with bonding κ and a field h only at s_2; see Figure 12. The partition function of the three site system can be written as

$$Z(\kappa, h, s_1, s_3) = \sum_{s_2} e^{\kappa(s_1 s_2 + s_2 s_3) + h s_2}. \tag{68}$$

Applying dedecoration, summing over site s_2, the field transforms, splits, and

propagates to the remaining sites. The pair-coupling also transforms and the energy shifts as well. The partition function after dedecoration is

$$Z(\kappa, h, s_1, s_3) = e^{\chi+\kappa'(s_1 s_3)+h'(s_1+s_3)}. \tag{69}$$

Here, χ is related to g mentioned previously by $\chi = \log g$. Now, any arbitrary spin function $\mathcal{F}$ can be expanded in terms of interactions between sites as

$$\mathcal{F} = \sum_a K_a s_a, \tag{70}$$

where s_a is the product of sites associated with interaction K_a. The s_a for pair-coupling is nearest neighbor sites and for the field it is single site interaction. The spin products s_a form a complete, orthogonal basis in the space of spin functions. This property can be used to invert Eq. (70) to yield,

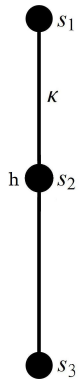

Figure 12. Three site system with bonding κ everywhere and field h only at site s_2

$$K_a = 2^{-n} \sum_{\{s\}} s_a \mathcal{F}, \tag{71}$$

where n stands for the number of lattice sites. Using Eq. (71) the renormalized

interactions are

$$\chi(\kappa,h)=\frac{1}{4}\sum_{s_1}\sum_{s_3}\log Z, \tag{72}$$

$$\kappa'(\kappa,h)=\frac{1}{4}\sum_{s_1}\sum_{s_3}s_1s_3\log Z, \tag{73}$$

$$h'(\kappa,h)=\frac{1}{4}\sum_{s_1}\sum_{s_3}s_1\log Z, \tag{74}$$

with the explicit representation in relation with how we previously defined these parameters given as

$$g(\kappa,h)=e^{\chi(\kappa,h)}=\sqrt{2\mathrm{Cosh}h}(2\mathrm{Cosh}4\kappa+2\mathrm{Cosh}2h)^{\frac{1}{4}}, \tag{75}$$

$$\kappa'(\kappa,h)=-\log[(\sqrt{2\mathrm{Cosh}h})(2\mathrm{Cosh}4\kappa+2\mathrm{Cosh}2h)^{-\frac{1}{4}}], \tag{76}$$

$$h'(\kappa,h)=\frac{1}{4}\log[(1+e^{2h+4\kappa})(e^{2h}+e^{4\kappa})^{-1}]. \tag{77}$$

The results in Eqs. (75), (76), and (77) are the dedecoration transformation results of a linear Ising spin lattice with a field acting only on sites being dedecorated and they will be used to resolve the hierarchical diamond system. Unlike linear Ising chains, which have the same connectivity for all sites, the process of how fields split and propagate in the hierarchical model depend on the varying connectivity of sites of lattice L_l. The problem of field splitting is fully defined in dedecorating hierarchical Ising systems by considering an example of the L_4 lattice dedecorated to L_3 and constructing a solution of the partition function of the system using recursion.

Application of dedecoration to the most general system of the hierarchical Ising model with an external field requires the notation h_k for the field site interaction parameters. The subscript k denotes a field at a site with 2^k connecting neighbors; using this notation, starting lattice L_l will have $l-1$ fields. Consider lattice L_4 with nearest neighbor interaction κ everywhere and fields h_1, h_2, and h_3; see Figure 13. The partition function for this system is $Z_4(\kappa,h_1,h_2,h_3)$.

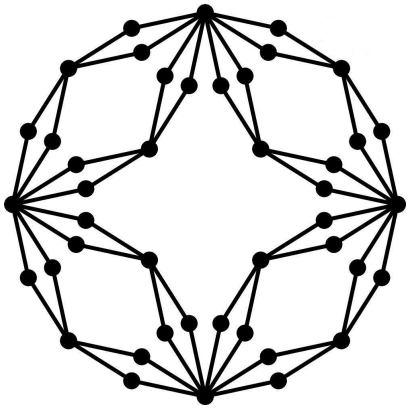

Figure 13. Hierarchical lattice L_4

One step of dedecoration requires a summation over all sites with two nearest neighbors to obtain L_3; see Figure 6. The sites with four neighbors become sites with two neighbors and the sites with eight neighbors become sites with four neighbors. One step of dedecoration to L_3 produces the renormalized bonding interaction $\kappa''(\kappa, h) = 2\kappa'(\kappa, h)$ everywhere and shift in the energy $g'(\kappa, h) = g^2(\kappa, h)$ due to the doubling of bonds; see Section 3.3.1. The dedecoration also produces two fields in the system

$$h'_1 = h_2 + 4h'(\kappa, h_1), \tag{78}$$

$$h'_2 = h_3 + 8h'(\kappa, h_1). \tag{79}$$

The resulting renormalized fields after dedecoration at the remaining sites are given by h'_k. The connecting piece in both Eqs. (78), (79) is $h'(\kappa, h_1)$ and it is the linear dedecoration transformation of field parameter h; see Eq. (77). Note, the two fields h'_1, h'_2 are not equivalent; the renormalized field at any site depends on both the connecting neighboring sites and the field that originally existed at the site. With this notation for any starting lattice L_l with $l-1$ fields the following renormalization field equation is

$$h'_k = h_{k+1} + 2^{k+1}h'(\kappa, h_1). \tag{80}$$

One iteration applied to partition function $Z_4(\kappa, h_1, h_2, h_3)$ gives

$$Z_4(\kappa, h_1, h_2, h_3) = G_3(\kappa, h_1) Z_3(\kappa'', h_1', h_2'). \tag{81}$$

Recall that G comes from a shift in energy upon dedecoration and this time it is related to the new $g(\kappa, h)$, i.e. $G_{l-1} = {g'}^{n_{l-1}^b} = g^{2\, n_{l-1}^b}$. The general partition function Z_l with $l-1$ fields after one step of dedecoration is

$$Z_l(\kappa, h_1, h_2, h_3, ..., h_{l-1}) = G_{l-1}(\kappa, h_1) Z_{l-1}(\kappa'', h_1', h_2', h_3', ..., h_{l-2}'). \tag{82}$$

The result of Eq. (82) completes the general analysis of hierarchical models with external fields. In practice we start with uniform magnetic field, but this property is not invariant under renormalization, which is rather unusual and more general than the method described in previous chapters.

3.3.4 The Complex Constants and Probabilities of Energy and Magnetization

The probability of finding the system in configuration S_l is given by

$$\mathcal{P}_l(S_l) = \frac{e^{\mathcal{H}_l(S_l, \kappa, h)}}{Z_l(\kappa, h)}. \tag{83}$$

The probability of finding the system in a state with magnetization M_0 is

$$\mathcal{P}_l(M_0) = \frac{\sum_{S_l} \delta_{M_0, M} e^{\mathcal{H}_l(S_l, \kappa, h)}}{Z_l(\kappa, h)}. \tag{84}$$

Where $M = \sum_i s_i$. The δ-function ensures that only those spin configurations that match the desired magnetization, M_0, survive the sum giving the desired probability. The probability of finding the system in a state with pair-coupling energy I_0 is

$$\mathcal{P}_l(\mathrm{I}_0) = \frac{\sum_{S_l} \delta_{\mathrm{I}_0, \mathrm{I}} e^{\mathcal{H}_l(S_l, \kappa, h)}}{Z_l(\kappa, h)}. \tag{85}$$

Where $\mathrm{I} = \sum_{\langle i,j \rangle} s_i s_j$. In general Eqs. (84) and (85) are cumbersome to calculate if the summations are carried out by brute force computation. Even in a computational routine brute force counting is numerically inefficient since the calculations

are usually repeated numerous times. A more efficient approach is giving by a complex transformation of the probability equations.

The Kronecker δ-function can be represented as a sum of exponentials. Consider two variables x, y that assume all integer values $0, 1, 2, \ldots, N$ for some max value N; these integers repeat in range $n = N+1$. For y fixed, the general complex transformation of $\delta_{x,y}$ is then given as

$$\delta_{x,y} = \frac{1}{n} \sum_{k=0}^{n-1} e^{2\pi i k \frac{x-y}{n}}. \tag{86}$$

If the variables $\delta_{x,y} = \delta_{0,x-y}$ do not initially assume values $0, 1, 2, \ldots, N$ then they can be shifted and scaled to do so. In the following applications of this transformation all variables denoted with primes are variables that need to be shifted and scaled to satisfy the requirement of being subsequent integers.

We can write

$$\delta_{M_0',M'} = \frac{1}{n} \sum_{k=0}^{n-1} e^{2\pi i k \frac{M_0'-M'}{n}}, \tag{87}$$

with $n = n_l^s + 1$, and M_0', M' defined as $M_0' = \frac{M_0+n_l^s}{2}$ and $M' = \frac{\sum_i s_i+n_l^s}{2}$ which accounts for the fact that the value of magnetization can be negative and that it takes steps of two in Ising models. The pair-coupling energy, I_0, can also assume negative values like magnetization. However, in the pair-coupling energy transform $n = n_l^b + 1$ and the energy takes steps of four, not two, so $\mathrm{I}_0', \mathrm{I}'$ are instead defined as $\mathrm{I}_0' = \frac{\mathrm{I}_0+n_l^b}{4}, \mathrm{I}' = \frac{\sum_{\langle i,j \rangle} s_i s_{i+1}+n_l^b}{4}$.

Application of the magnetization and pair-coupling energy complex transformations to Eqs. (84) and (85) allows manipulation of the sums to write the numerators in the probability equations as partition functions with shifted interaction parameters. The probabilities for magnetization and pair-coupling energy

are now expressed as

$$\mathcal{P}_l(M_0) = \frac{1}{n_l^s + 1} \sum_{k=0}^{n_l^s} e^{\pi i k \frac{M_0}{n_l^s+1}} \frac{Z_l(\kappa, h - \frac{\pi i k}{n_l^s+1})}{Z_l(\kappa, h)}, \tag{88}$$

$$\mathcal{P}_l(\mathrm{I}_0) = \frac{1}{n_l^b + 1} \sum_{k=0}^{n_l^b} e^{\pi i k \frac{\mathrm{I}_0}{2(n_l^b+1)}} \frac{Z_l(\kappa - \frac{\pi i k}{2(n_l^b+1)}, h)}{Z_l(\kappa, h)}. \tag{89}$$

Numerically, Eqs. (88), (89) allow us to compute the full probability distributions recursively. See Figure 14 for the result of such a calculation.

List of References

[1] E. Ising, "Beitrag zur Theorie des Ferromagnetismus," *Zeitschrift fur Physik*, 1925.

[2] D. V. Schroeder, *An Introduction to Thermal Physics.* Boston, Massachusetts, United States of America: Addison Wesley Longman, 2000.

[3] K. Huang, *Statistical Mehcanics, 2nd. edn.* Hoboken, New Jersey, United States of America: John Wiley and Sons, INC., 1987.

[4] L. E. Reichl, *A Modern Course in Statistical Physics.* Austin, Texas, United States of America: University of Texas Press, 1980.

[5] L. D. Landau and E. M. Lifshitz, *Statistical Physics 3rd Edition Part 1.* The Boulevard, Langford Lane, Kidlington, Oxford: Butterworth-Heinemann, 1980.

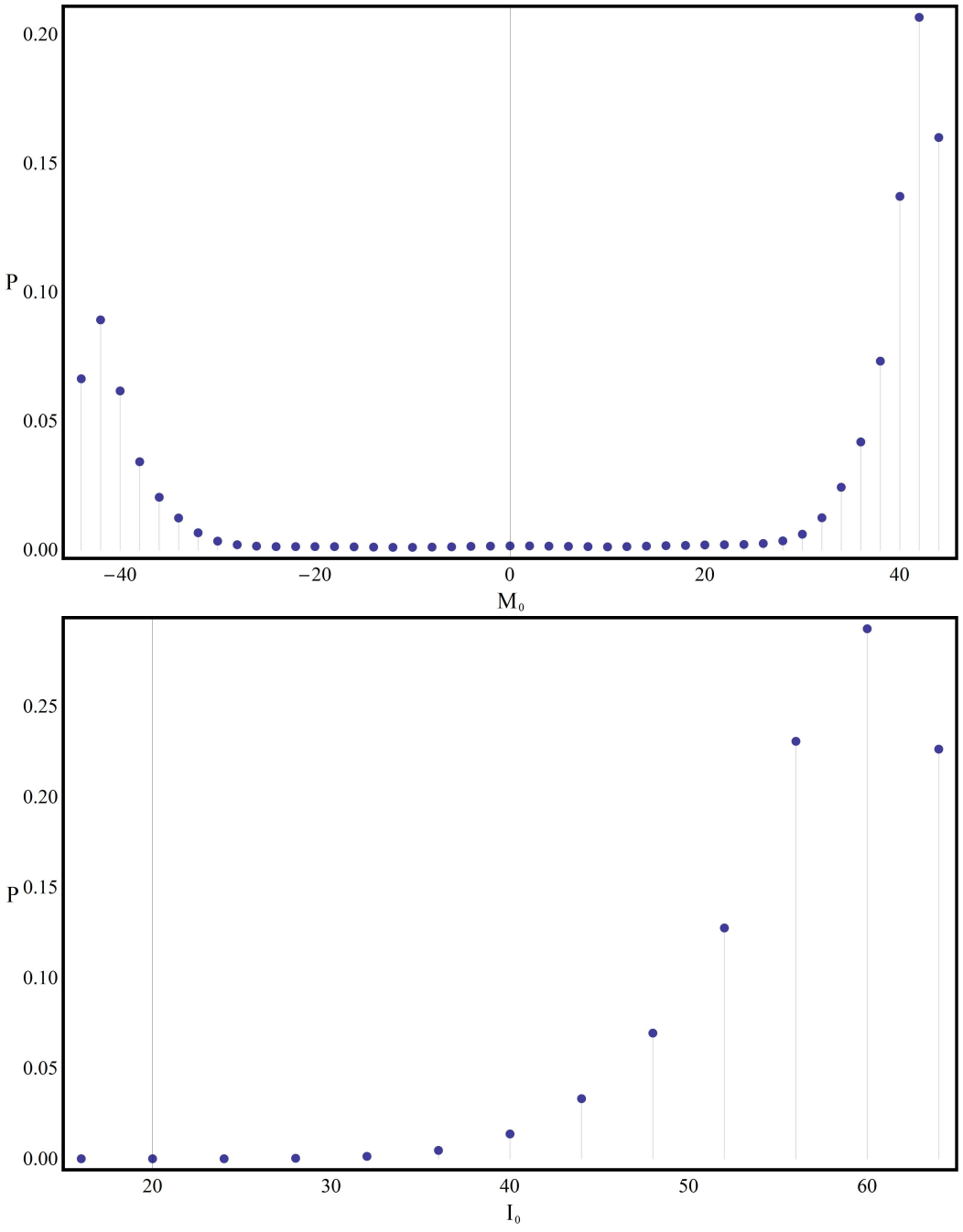

Figure 14. The probability of magnetization and pair-coupling energy for a L_4 hierarchical Ising lattice with 64 bonds and 44 sites; $\kappa = 0.8$, $h = 0.01$.

CHAPTER 4

The q-state Potts Model

The Potts model is a generalization of the Ising model described by Renfrey Potts in his 1951 Ph.D. thesis [1]. Like the Ising model, the Potts model features nearest-neighbor interactions. Unlike the Ising model, which could only have site variables assume two discrete states, the Potts model allows $s_i = 1, 2, ..., q$ discrete states for configuration S_l. The rest of this dissertation restricts itself almost exclusively to hierarchical diamond lattices; see Figures 4, 5, 6. When the hierarchical Potts diamond lattice with field is covered, a step back is made to linear lattices to develop the renormalization group equations needed for the hierarchical lattice analysis. With the goal in mind of constructing quantities suitable for both numerically exact and Monte Carlo computation, we consider the heat capacity in addition to the probability distributions of pair-coupling energy and the order-like parameter of q-state Potts Hamiltonian used.

4.1 The Hierarchical q-state Potts Diamond

Generalizing the hierarchical Ising diamond equations for a q-state model allows us to develop the renormalization group equations of the hierarchical Potts diamond [2]. These equations for the q-state Potts system can be obtained by constructing the transfer matrix with a Hamiltonian of the hierarchical Potts diamond that is invariant under the RG transformation. The following Potts bond Hamiltonian for any lattice level l and variables $s_i = 1, \ldots, q \in S_l$ satisfies this

requirement,

$$H_l^q(s_1, s_2, w, \kappa, \lambda, h) = w + \kappa\Theta(s_1 \neq s_2) + \lambda[\Theta(s_1 = 1\,\&\,s_2 > 1) + \Theta(s_2 = 1\,\&\,s_1 > 1)] + \frac{1}{2}h[\Theta(s_1 = 1) + \Theta(s_2 = 1)]. \quad (90)$$

where $\Theta(p) = 1(0)$ if p is true(false). Here κ and h are the previous pair and external field interactions and λ is a second pair interaction, which is generated by the dedecoration operation as soon as the field h differs from zero and $q > 2$. Finally, the parameter w reflects the freedom in choice of the zero of energy. It will be fixed by convention and will generate the self-energy term in the scaling relation for the free energy. The $q = 2$ case can be related to the Ising model by means of a simple transcription. The transfer matrix for integral q is constructed as a $q \times q$ matrix that can be conveniently expressed in Boltzmann weight form [3] as

$$T^q(a, b, c, d) = \begin{bmatrix} a & b & b & b & b & ... & b \\ b & d & c & c & c & ... & c \\ b & c & d & c & c & ... & c \\ b & c & c & d & c & ... & c \\ . & . & . & . & . & . & . \\ . & . & . & . & . & . & . \\ b & c & c & c & c & c & d \end{bmatrix}. \quad (91)$$

Both Eqs. (90) and (91) have four parameters.

4.2 Potts Lattice Dedecoration in Zero Field

Dedecoration of the Potts diamond Hamiltonian in zero field reduces Eq. (90) to only one coupling constant, κ. To obtain the conventional form of the Potts model for Eq. (91) in the absence of a field we choose $a = d = 1$, and $b = c =$

$\exp(\kappa)$:

$$T^q(a) = \begin{bmatrix} 1 & b & b & b & b & ... & b \\ b & 1 & b & b & b & ... & b \\ b & b & 1 & b & b & ... & b \\ b & b & b & 1 & b & ... & b \\ . & . & . & . & . & . & . \\ . & . & . & . & . & . & . \\ b & b & b & b & b & b & 1 \end{bmatrix}. \tag{92}$$

Unity along the diagonal in Eq. (92) corresponds to the $w = 0$ convention for Eq. (90). The dedecoration, or renormalization group, equations in the absence of an external field are derived by taking the product of Eq. (92) with itself followed by factorization of the resultant matrix back to standard form. As discussed in Section 2.1, the RG transformation of the transfer matrix consists of matrix squaring, *i.e.*, dedecoration, squaring of the resulting matrix elements, *i.e.*, bond doubling, and imposing the zero of energy convention:

$$g'(b,q) = (1 + (q-1)b^2)^2, \tag{93}$$

$$b''(b,q) = \left(\frac{b(2 + (q-2)b)}{1 + (q-1)b^2}\right)^2, \tag{94}$$

where g' comes from the pair-site dedecoration energy shift and b'' is the renormalized Boltzmann weighted pair-coupling parameter. Similar to the Ising analysis, see Section 3.3.1, we can write $b_1(b,q) = b''(b,q)$. The transformation has a fixed point

$$b_1(b_c,q) = b_c = \left(1 + \frac{2(\frac{2}{3})^{\frac{1}{3}}q}{r(q)} + \frac{r(q)}{2^{\frac{1}{3}}3^{\frac{2}{3}}}\right)^{-1}, \tag{95}$$

with

$$r(q) = (9q^2 + \sqrt{3}\sqrt{-32q^3 + 27q^4})^{\frac{1}{3}}. \tag{96}$$

Note that we can generalize the model and consider q as a continuous variable. We have not explored the simulation of lattices with continuous q and will refrain from doing so. The method we use, and as explained in detail below, does not lend itself for that purpose.

4.2.1 Hierarchical Diamond Lattice Total Energy and Heat Capacity

The partition function, the energy, and the heat capacity of the hierarchical q-state Potts model in zero field are conveniently expressed in Boltzmann weight form. Let $Z_l^q(b)$ be the partition of the hierarchical lattice of level l, state q. The partition function satisfies the following recursion relation

$$Z_l^q(b) = G_{l-1}^q(b) Z_{l-1}^q(b_1) = {g'}^{n_{l-1}^b}(b,q) Z_1^q(b_1). \tag{97}$$

The reduced free energy $F_l^q = \log Z_l^q$ satisfies the scaling relation

$$F_l^q(b) = J_{l-1}^q(b) + F_{l-1}^q(b_1), \tag{98}$$

where

$$J_{l-1}^q(b) = n_{l-1}^b \log g'(b,q). \tag{99}$$

From the free energy the thermodynamic quantities of interest follow by taking derivatives of F with respect to b,

$$F_l^{q(1)} = {J_{l-1}^q}^{(1)} + {F_{l-1}^q}^{(1)} {b_1}^{(1)}, \tag{100}$$

$$F_l^{q(2)} = {J_{l-1}^q}^{(2)} + {F_{l-1}^q}^{(2)} ({b_1}^{(1)})^2 + {F_{l-1}^q}^{(2)} {b_1}^{(2)}, \tag{101}$$

where all superscripts in parentheses denote first and second derivatives with respect to the arguments b and b_1. With Eqs. (100) and (101), the total energy and heat capacity of lattice l and state parameter q are

$$U_l^q = \frac{\partial F_l^q}{\partial \log b} = b F_l^{q(1)}, \tag{102}$$

$$C_l^q = \frac{\partial^2 F_l^q}{\partial (\log b)^2} = b(b F_l^{q(2)} + F_l^{q(1)}). \tag{103}$$

To compare to Monte Carlo simulations in Chapter 5 we once again only use finite lattices. In calculations, the derivatives of the free energy can all be predefined and calculated numerically; see Appendix A.

The q-state Potts model has specific heat that diverges at the critical point for q sufficiently large. We expect that this makes Monte Carlo computations for large values of q more sensitive to correlations in the RNGs. Figures 15 and 16 shows results for both the total energy and heat capacity per bond with $q = 400$ for various large finite systems. Figure 17 shows the $q = 2$ Ising results for the heat capacity per bond for the same finite systems for comparison.

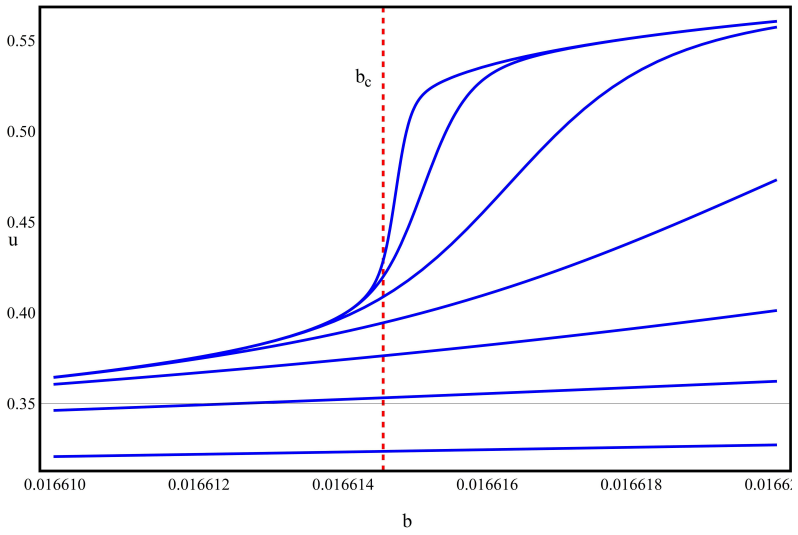

Figure 15. The total energy per bond $u = \frac{U}{n_l^b}$. This figure uses $q = 400$ and range the lattice level from $l = 6$,..., 12. The fixed value b_c for this selection of q is $b_c = 0.016615$.

4.3 Hierarchical Potts Diamond Lattice in a Field

We now consider the RG transformation of the hierarchical Potts model in a field. Using Eq. (90) and choosing $w = 0$, the following transfer matrix can be seen to have a structure that is invariant under renormalization,

$$T^q(a,b,c) = \begin{bmatrix} a & b & b & b & b & ... & b \\ b & 1 & c & c & c & ... & c \\ b & c & 1 & c & c & ... & c \\ b & c & c & 1 & c & ... & c \\ . & . & . & . & . & . & . \\ . & . & . & . & . & . & . \\ b & c & c & c & c & c & 1 \end{bmatrix}, \tag{104}$$

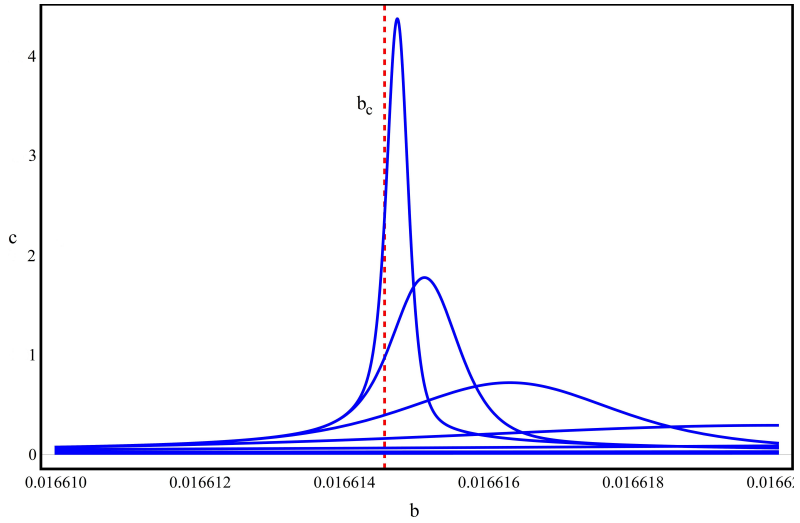

Figure 16. The heat capacity per bond $c = \frac{C}{n_l^b \times 10^3}$. The additional 10^3 in the denominator is purely for scaling. This figures uses $q = 400$ and range the lattice level from $l = 6$,..., 12. The fixed value b_c for this selection of q is $b_c = 0.016615$.

with

$$\begin{aligned} a &= e^h & b &= e^{\frac{1}{2}h+\kappa+\lambda} \\ c &= e^\kappa & d &= 1 \end{aligned} \tag{105}$$

We again remind the reader that we choose $d = 1$ as a convention.

For the case of a non-zero external field first, we derive the renormalization group equations for a linear chain; see Figures 1, 2, 3. Upon application of decoration, every other site gets summed over and the field of the summed sites propagates to the remaining sites. Each remaining site always gets contributions of the field from its two previous neighbors. Compared to the case of hierarchical lattices, this simplifies the renormalization group Eq. (80) in Section 3.3.3; here we find

$$h_1' = h + 2h'(\kappa, \lambda, h, q). \tag{106}$$

Recall that h_1' denotes the renormalized field interaction at a remaining site after

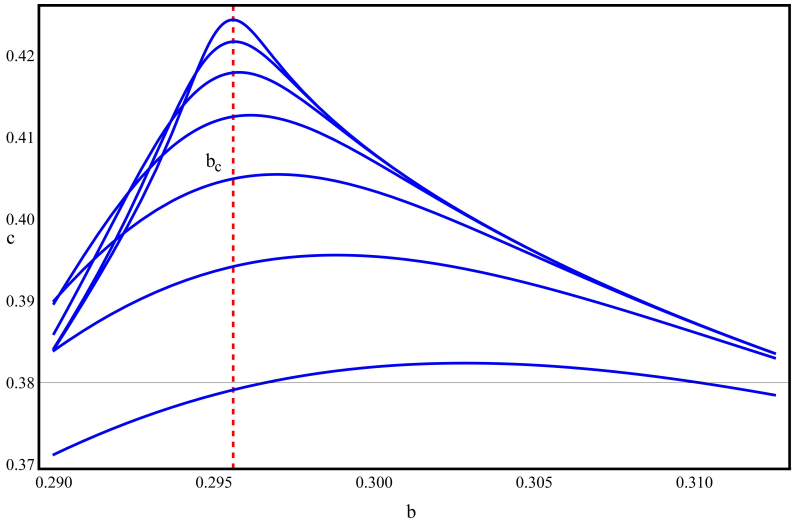

Figure 17. The heat capacity per bond, $c = \frac{C}{n_l^b}$, for the $q = 2$ Potts model. In this figure we range the lattice level from $l = 6$,..., 12. The fixed value b_c for this selection of q is $b_c = 0.295686$.

dedecoration with two neighbors. One application of dedecoration to transform L_l to L_{l-1} requires the product of Eq. (104) with itself and factorization to standard form. This process yields the linear Potts chain lattice renormalization group equations:

$$g(\kappa, \lambda, h, q) = 1 + (q-2)\, e^{2\kappa} + e^{h+2\kappa+2\lambda}, \tag{107}$$

$$\kappa'(\kappa, \lambda, h, q) = \log\left[\frac{e^{\kappa}\left(2 + (q-3)\, e^{\kappa} + e^{h+\kappa+2\lambda}\right)}{1 + (q-2)\, e^{2\kappa} + e^{h+2\kappa+2\lambda}}\right], \tag{108}$$

$$\begin{aligned}\lambda'(\kappa, \lambda, h, q) =& \frac{1}{2}\log\left[\frac{e^{h+2\kappa+2\lambda}\left(1 + e^{h} + (q-2)\, e^{\kappa}\right)^2}{1 + (q-2)\, e^{2\kappa} + e^{h+2\kappa+2\lambda}}\right] \\ &- \log\left[\frac{e^{\kappa}\left(2 + (q-3)\, e^{\kappa} + e^{h+\kappa+2\lambda}\right)}{1 + (q-2)\, e^{2\kappa} + e^{h+2\kappa+2\lambda}}\right] \\ &- \frac{1}{2}\log\left[\frac{e^{h}\left(e^{h} + (q-1)\, e^{2\kappa+2\lambda}\right)}{1 + (q-2)\, e^{2\kappa} + e^{h+2\kappa+2\lambda}}\right],\end{aligned} \tag{109}$$

$$h_1'(\kappa, \lambda, h, q) = \log\left[\frac{e^{h}\left(e^{h} + (q-1)\, e^{2\kappa+2\lambda}\right)}{1 + (q-2)\, e^{2\kappa} + e^{h+2\kappa+2\lambda}}\right]. \tag{110}$$

Combining Eqs. (106) and (110) gives the basic single site renormalization group equation of how sites transform in both the linear and hierarchical Potts lattices,

$$h'(\kappa,\lambda,h,q)=\frac{1}{2}\log\left[\frac{e^{h}+(q-1)\,e^{2\kappa+2\lambda}}{1+(q-2)\,e^{2\kappa}+e^{h+2\kappa+2\lambda}}\right]. \tag{111}$$

We remind the reader that pair-site dedecoration in hierarchical diamond lattices require the energy shift to be squared, and the pair-coupling to be doubled; this gives $g'=g^2$, $\kappa''=2\kappa'$, and $\lambda''=2\lambda'$. Additionally, we point out to the reader that the connectivity of neighbors in the hierarchical Potts diamond lattice is exactly the same as the hierarchical Ising diamond lattice. This implies that the Chapter 3 renormalization group equation result Eq. (80) for external fields in the hierarchical Ising diamond is also the correct field renormalization group equation in the hierarchical Potts diamond except the h' in Eq. (80) is now given by Eq. (111). The partition function for a q-state hierarchical Potts diamond lattice of level l with initially uniform pair-coupling and single-site interactions can now be calculated by starting the recursion with the following equation,

$$Z_l^q(\kappa,\lambda,h)=G_{l-1}^q(\kappa,\lambda,h)Z_{l-1}^q(\kappa'',\lambda'',h_1',h_2',h_3',...,h_{l-2}'), \tag{112}$$

where $G_{l-1}^q(\kappa,\lambda,h)=g'^{n_l^b}(\kappa,\lambda,h,q)$.

4.4 Hierarchical q-state Potts Model Probability Distributions

Using the partition function Eq. (112), the probability distributions of the hierarchical Potts diamond lattices can be constructed closely following the procedure used for the Ising model. We restrict analysis to $q\geq 3$ in what follows. The pair-coupling energy, I, with zero-field, from the Hamiltonian of Eq. (90) is

$$\mathrm{I}=\sum_{\langle i,j\rangle\in L_l}\Theta(s_i\neq s_j). \tag{113}$$

The probability of finding the system in a state with energy I_0 is

$$\mathcal{P}_l^q(\mathrm{I}_0)=\frac{\sum_{S_l}\delta_{\mathrm{I}_0,\mathrm{I}}e^{\mathcal{H}_l^q(S_l,\kappa)}}{Z_l^q(\kappa)}. \tag{114}$$

For $q \geq 3$ the energy distribution increases by steps of one. From Section 3.3.4 the complex transformation of the Kronecker delta allows Eq. (114) to be written as

$$\mathcal{P}_l^q(\mathrm{I}_0) = \frac{1}{n_l^b+1} \sum_{k=0}^{n_l^b} e^{2\pi i k \frac{\mathrm{I}_0}{n_l^b+1}} \frac{Z_l^q(\kappa - \frac{2\pi i k}{n_l^b+1})}{Z_l^q(\kappa)}, \tag{115}$$

with the partition functions given by Eq. (112) for zero-field. The order-like parameter, M, from Hamiltonian Eq. (90) is

$$M = \sum_{i=1}^{n_s} \Theta(s_i = 1). \tag{116}$$

The probability of finding the system in a state with given value of M_0 is

$$\mathcal{P}_l^q(M_0) = \frac{\sum_{S_l} \delta_{M_0,M} e^{\mathcal{H}_l^q(S_l,\kappa,\lambda,h)}}{Z_l^q(\kappa,\lambda,h)}. \tag{117}$$

For $q \geq 3$ this distribution also takes steps of one. By Section 3.3.4 the complex transformation then gives

$$\mathcal{P}_l^q(M_0) = \frac{1}{n_l^s+1} \sum_{k=0}^{n_l^s} e^{2\pi i k \frac{M_0}{n_l^s+1}} \frac{Z_l^q(\kappa,\lambda,h - \frac{2\pi i k}{n_l^s+1})}{Z_l^q(\kappa,\lambda,h)}, \tag{118}$$

with the partition functions given by Eq. (112). Note, if the field is taken as zero in Eq. (118), the shift acting on the field interaction term still remains. In Figure 18 we show probabilities for the L_4 lattice with $q = 3$ evaluated at the critical point using Eqs. (115) and (118). In practice, we apply recursion to the partition functions until the L_2 lattice. The L_2 lattice is a sufficient stopping point because it is the first lattice in the dedecoration process where all site parameters will be equal to each other no matter what the starting conditions; brute force calculation of the partition function is easily applicable at the L_2 lattice. Note, computing the corresponding partition function of the L_2 lattice by brute force counting will still take time proportional to q^4. This becomes long for large q and can be avoided by writing the partition function for the L_2 lattice as a polynomial in q; see Appendix B for how this is done for zero-field.

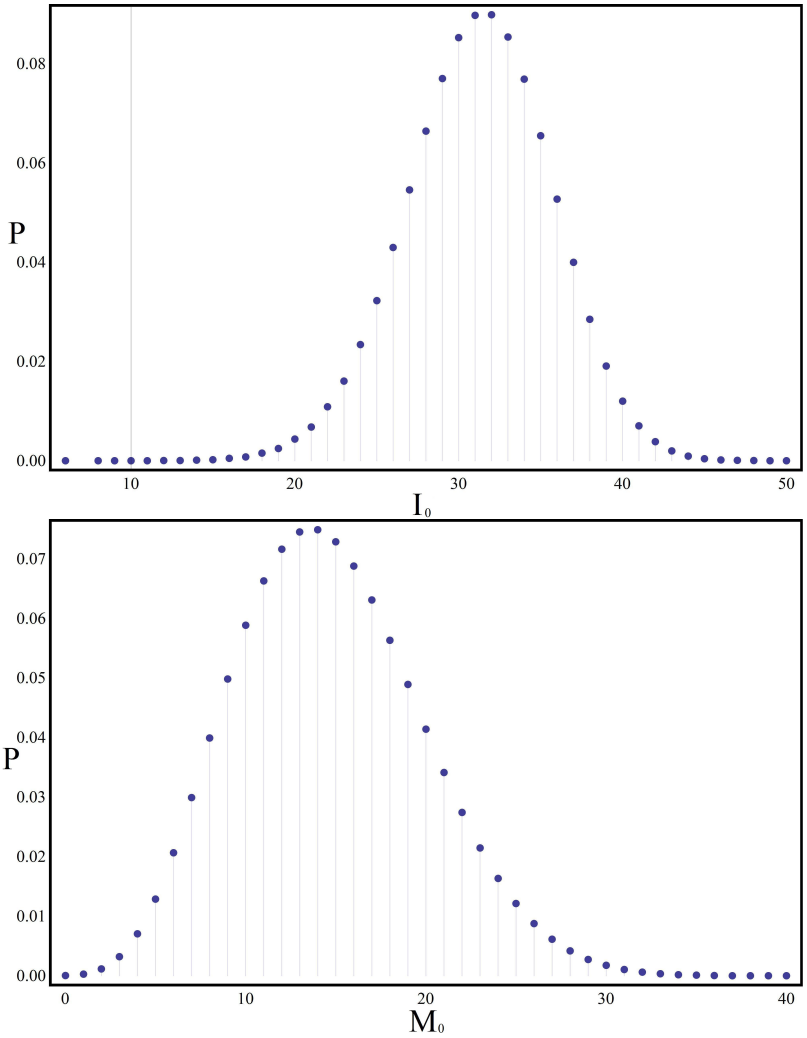

Figure 18. The $q = 3$ probability distributions for a L_4 hierarchical q-state Potts diamond lattice at the critical point; $\kappa_c = \frac{1}{2}\log b_c = -0.693147$, $\lambda = h = 0$.

List of References

[1] R. Potts, "Some Generalized Order-Disorder Transformations," *Mathematical Proceedings*, vol. 48, 1952.

[2] M. E. J. Newman and G. T. Barkema, *Monte Carlo Methods in Statistical Physics*. Oxford, New York, United States of America: Oxford University Press, 1999.

[3] M. P. Nightingale, "Private Communication."

CHAPTER 5

Monte Carlo Simulation of the Hierarchical q-state Potts Diamond Lattice at the Critical Point

Random numbers are used in applications of Monte Carlo (MC). However, for practical purposes we are limited to algorithms that can generate numbers that only appear to be random; these algorithms are called Pseudo-Random Number Generators (PRNGs). There are many different types of these generators [1]. A PRNG after being appropriately seeded, recursively generates a sequence of numbers that have the properties of random numbers. We shall not attempt to provide a definitive definition of what a random number is; let us just say that the sequence of numbers $(r_1, r_2, ..., r_n)$ should contain no information about r_{n+1} for "reasonable" choice of n. In pseudo-random number generators, r_{n+1} is always determined by its predecessors and therefore cannot be a truly random number. Although the numbers produced by PRNGs are "pseudo-random numbers" we will simply refer to both the generator and output as "Random Number Generator" (RNG) and "random numbers" instead. If these random numbers are sufficiently correlated, the Monte Carlo will have systematic errors in addition to unavoidable statistical ones.

The bias introduced by correlated random numbers is not a problem when it is smaller than the statistical error of a particular computation. However, as more compute cycles become available, these statistical errors decrease so that the demands on the quality of the RNG increase. In practice, RNGs are subjected to various test suites [2] that have been developed in the past. We are interested in adding yet another random number generator test to the standard battery.

Thermal and magnetic quantities in the hierarchical q-state Potts diamond lattice can be expressed as sums of correlation functions that diverge on approach

of the critical point in an infinite system. In the finite system, which are the only ones where Monte Carlo is applicable, these quantities have no divergences. Nonetheless, because of the incipient divergences, finite system near criticality are highly sensitive to correlations introduced by a bad random number generator. It is this property we intend to exploit.

In this chapter we discuss the details of a Monte Carlo algorithm with which one can compute estimates of observables like the heat capacity. These estimates are to be compared with the theoretical values computed by the methods discussed in the previous chapters. The probability distributions discussed previously are also estimated by constructing histograms.

5.1 Monte Carlo Simulation of The Hierarchical q-state Potts Diamond Lattice by Direct Sampling

To sample the Boltzmann distribution one can use the Metropolis-Hastings (MH) algorithm. However, there is an inherent problem in using such algorithms, a problem that is shared by other more sophisticated algorithms that have been designed with the problem of critical slowing down [3]. If any non-trivial Markov process is used to sample the Boltzmann distribution, subsequent configurations will be correlated. This typically reduces the efficiency of a calculation, while also, burn-in is required because an initial configuration may be chosen with a probability that does not correspond to equilibrium.

Hierarchical lattices have the unique feature that the configurations they support can be sampled directly by the decoration procedure that generates the lattice geometry. At each step of decoration, at most, two frozen nearest neighbors determine the probability of the state of the site added next. In this way one can generate lattice configurations of arbitrary size.

5.1.1 The Direct Sampling Algorithm for the Zero Field Hierarchical q-State Potts Diamond lattice

The very first site of our lattice of Potts variables, s_1, has no neighbors, so that each state has equal probability

$$\mathcal{P}(s_1) = \frac{1}{q}. \tag{119}$$

Once the first site is generated according to Eq. (119) the second site is generated in the absence of a magnetic field with probability

$$\mathcal{P}(s_2|s_1) = \frac{b^{\Theta(s_1 \neq s_2)}}{\sum_{s_2'} b^{\Theta(s_1 \neq s_2')}}. \tag{120}$$

Here, we remind the reader that $b = e^{\kappa}$ is the Boltzmann weight associated with the pair-coupling; see Section 4.2. After this, all new sites decorate an already existing bond in a state defined by s_1 and s_2; the new state of the decorating site is s_3, which is chosen with probability

$$\mathcal{P}(s_3|s_1, s_2) = \frac{b^{(\Theta(s_1 \neq s_3) + \Theta(s_3 \neq s_2))}}{\sum_{s_3'} b^{(\Theta(s_1 \neq s_3') + \Theta(s_3' \neq s_2))}}. \tag{121}$$

Using these probabilities one can build any lattice one site at a time; see Figures 4, 5, and 6.

The Implementation of the Direct Sampling Algorithm

This subsection discusses how the sampling described in the previous section is implemented in detail; the reader may skip to section 5.2 to continue with the standard error analysis techniques we propose for the RNG test. Consider readily available the sequence of random numbers $(r_1, r_2, ..., r_n)$ from the U(0,1) distribution.

1. Use r_1 to determine state of s_1 with Eq. (119).

2. Use r_2 against Eq. (120) to determine state of s_2

- If $r_2 > \mathcal{P}(s_2 = s_1|s_1)$ then state of s_2 is same as s_1.
- If $r_2 < \mathcal{P}(s_2 = s_1|s_1)$ use r_3 to choose s_2 from $q-1$ possibilities.

3. Determine s_3 with Eq. (121).

- If $s_1 = s_2$, $\mathcal{P}(s_3 = s_1|s_1, s_2) = \mathcal{P}(s_3 = s_2|s_1, s_2)$.
  - If $r_3 > \mathcal{P}(s_3 = s_1|s_1, s_2)$ then state of s_3 is same as s_1,s_2.
  - If $r_3 < \mathcal{P}(s_3 = s_1|s_1, s_2)$ use r_4 to choose s_3 from $q-1$ possibilities.
- If $s_1 \neq s_2$, $\mathcal{P}(s_3 = s_1|s_1, s_2) = \mathcal{P}(s_3 = s_2|s_1, s_2)$.
  - If $r_4 > \mathcal{P}(s_3 = s_1|s_1, s_2)$ then state of s_3 is same as s_1 or s_2.
  - If $r_4 < \mathcal{P}(s_3 = s_1|s_1, s_2)$ use r_5 to choose s_3 from $q-2$ possibilities.

All newly included sites after s_2 will always only have two nearest neighbors like s_3.

5.2 Standard Error Analysis

Using Monte Carlo we want to calculate the expectation value $\langle Q \rangle$ of some observable Q. The statistical ensemble average of a system of all states allowed, μ, defines $\langle Q \rangle$,

$$\langle Q \rangle = \frac{\sum_\mu Q_\mu e^{\mathcal{H}_\mu}}{\sum_\mu e^{\mathcal{H}_\mu}}. \tag{122}$$

However, we assume that during a Monte Carlo run the system will not pass through every possible state. With MC direct sampling we generate configurations with a probability given by the Boltzmann distribution [4]. The ensemble average of the expectation value can then be written as a time average. The unbiased estimator, $\overline{Q}$, of this expectation value, $\langle Q \rangle$, is

$$\overline{Q} = \frac{1}{t} \sum_{i=1}^{t} Q_i. \tag{123}$$

Note, as $t \to \infty$ we have the property that $\overline{Q} = \langle Q \rangle$. From this average we calculate the standard deviation, σ, of the observable,

$$\sigma = \sqrt{\frac{1}{t-1}\sum_{i=1}^{t}(Q_i - \overline{Q})^2}. \tag{124}$$

Direct sampling yields independent realizations of observable Q, and for large t, $\overline{Q}$ is normally distributed around $\langle Q \rangle$ according to the central limit theorem. The probability that $\overline{Q}$ exceeds deviation Δ from $\langle Q \rangle$ is

$$\mathcal{P}(|\,\overline{Q} - \langle Q \rangle| > \Delta) = 1 - \mathrm{erf}\left(\frac{\Delta}{\sqrt{2}\sigma}\right). \tag{125}$$

These standard techniques can be applied to any observable to determine whether observed estimates deviate significantly from their expected values.

5.3 The Probability Distributions and χ^2

To estimate whether the estimates obtained for a whole probability distribution agree with what is theoretically expected, the usual χ^2 statistic is an obvious choice:

$$\chi^2 = \sum_{k=1}^{w} x_k^2. \tag{126}$$

If the x_k are independent, standard normal stochastic variables, χ^2 is distributed according to the χ^2 distribution of w degrees of freedom. Consider during an MC run consisting of t observations we construct a histogram. The number of times that an observable assumes the value associated with the kth bin of this histogram is t_k. The corresponding distribution is the binomial distribution with average $p_k t$ and variance $p_k t(1 - p_k)$. Here, p_k is the probability of landing in bin k. The chi-square statistic is then

$$\chi^2 = \sum_{k=1}^{w} \frac{(t_k - p_k t)^2}{p_k t(1 - p_k)}. \tag{127}$$

The problem in applying this statistic to the bins is that many correspond to extremely improbable events. The condition of normality for applicability of

the χ^2-distribution is not satisfied for such bins. To deal with this problem we introduce super-bins formed by combining sufficiently many neighboring bins until the combined bin count exceeds the expected RMS error by a sizable factor for each bin. In practice, we use the following condition as it guarantees a normal distribution of the bin counts. We define $\mathcal{N}[\mu, \sigma^2]$ as the normal distribution with average μ and variance σ^2. Each term in Eq. (127) must then be distributed like $\mathcal{N}[tp_k, tp_k(1-p_k)]$ for all $k = 1, \ldots, w$. We treat this condition as being satisfied to a sufficient degree of accuracy when for all histogram bins we have: $tp_k - 3\sqrt{tp_k(1-p_k)} > 0$ and $tp_k + 3\sqrt{tp_k(1-p_k)} < t$, *i.e.*, if $t > 9\text{Max}[(1-p)/p, p/(1-p)]$.

5.4 The Hierarchical q-state Potts Diamond Model Random Number Generator Test: Subsequent Research

The actual development of the q-state hierarchical Potts diamond lattice RNG test is the next step. A portable version of the test must be developed and only require the input of a RNG to operate. This will allow easy testing of various types of generators from basic linear congruential generators to generators that are standard in language environments like FORTRAN 90. The test needs to be used with simple well-known faulty RNGs as a check of consistency. Once that has been accomplished, the test will need to be applied to generators that are still used currently and regarded as "good" so that real conclusions can be drawn on how successful the test works.

List of References

[1] Wikipedia. "List of random number generators." apr 2014. [Online]. Available: http://en.wikipedia.org/wiki/List_of_random_number_generators

[2] TestU01. "Testu01." aug 2009. [Online]. Available: http://www.iro.umontreal.ca/~simardr/testu01/tu01.html

[3] D. L. A.M. Ferrenburg and Y. Wong, "Monte Carlo simulations: Hidden errors from 'good' random number generators," *Physical Review*, vol. 69, 3382, 1992.

[4] M. E. J. Newman and G. T. Barkema, *Monte Carlo Methods in Statistical Physics*. Oxford, New York, United States of America: Oxford University Press, 1999.

APPENDIX A

: The Energy and Heat Capacity Chain Rule Method

Consider the free energy and first derivative of the recursive free energy of the q-state Potts model with respect to internal argument b. We drop the superscript dependence on q to simplify the notation,

$$F_l(b) = J_l(b) + F_{l-1}(b_1), \tag{A.1}$$

$$F_l^{(1)}(b) = J_l^{(1)}(b) + {b_1}^{(1)}(b) F_{l-1}^{(1)}(b_1). \tag{A.2}$$

We write Eq. (A.2) in the following form,

$$F_l^{(1)}(b) = \frac{\partial}{\partial b} J_l(b) + \frac{\partial b_1}{\partial b} \frac{\partial}{\partial b_1} F_{l-1}(b_1). \tag{A.3}$$

Recursively iterate Eq. (A.3) once to see the trend,

$$F_l^{(1)}(b) = \frac{\partial}{\partial b} J_l(b) + \frac{\partial b_1}{\partial b} \frac{\partial}{\partial b_1} \Big(J_{l-1}(b_1) + F_{l-2}(b_2) \Big). \tag{A.4}$$

Continue to reiterate Eq. (A.4) and focus on the coefficients J. We then have

$$F_l^{(1)}(b) = \frac{\partial}{\partial b} J_l(b) + \frac{\partial b_1}{\partial b} \frac{\partial}{\partial b_1} \Big(J_{l-1}(b_1) + \Big(J_{l-2}(b_2) + ... \Big) \Big). \tag{A.5}$$

Distribute the derivatives,

$$F_l^{(1)}(b) = \frac{\partial}{\partial b} J_l(b) + \frac{\partial b_1}{\partial b} \frac{\partial}{\partial b_1} J_{l-1}(b_1) + \frac{\partial b_1}{\partial b} \frac{\partial}{\partial b_1} J_{l-2}(b_2) + ... \tag{A.6}$$

On the final term shown we use chain rule to rewrite the expression Eq. (A.6) as,

$$F_l^{(1)}(b) = \frac{\partial}{\partial b} J_l(b) + \frac{\partial b_1}{\partial b} \frac{\partial}{\partial b_1} J_{l-1}(b_1) + \frac{\partial b_1}{\partial b} \frac{\partial b_2}{\partial b_1} \frac{\partial}{\partial b_2} J_{l-2}(b_2) + ... \tag{A.7}$$

In an infinite system the final term of the sum would be pushed infinitely far away and one could approximate the energy by including more J terms in the sum.

However, in a finite system the dedecoration and therefore the sum of terms must end. The L_1 two site lattice is the final stop point of finite dedecoration. Recursion with Eq. (A.7) in a finite system gives

$$F_l^{(1)}(b) = \frac{\partial}{\partial b} J_l(b) + \frac{\partial b_1}{\partial b}\frac{\partial}{\partial b_1} J_{l-1}(b_1) + \frac{\partial b_1}{\partial b}\frac{\partial b_2}{\partial b_1}\frac{\partial}{\partial b_2} J_{l-2}(b_2) + ... \\ ... + \frac{\partial b_1}{\partial b}\frac{\partial b_2}{\partial b_1}\frac{\partial b_3}{\partial b_2} \times ... \times F_1^{(1)}(b_k). \quad \text{(A.8)}$$

The final term is the brute force derivative of the free energy of the L_1 system with respect to b_k which is the final dedecorated coupling parameter of the lattice,

$$F_1^{(1)}(b_k) = \frac{\partial}{\partial b_k} \log\Big[Z_1(b_k)\Big]. \quad \text{(A.9)}$$

The total energy of the system is now written in terms of derivatives of quantities that can be pre-defined. The partial derivatives, $\partial b_1/\partial b$, $\partial b_2/\partial b_1$, etc, are all the same derivative of b_1 w.r.t. to b evaluated at a new Boltzmann pair-coupling point. Recall, the renormalized expression for b_1,

$$b_1(b,q) = \left(\frac{b\big(2 + b(q-2)\big)}{1 + b^2(q-1)}\right)^2. \quad \text{(A.10)}$$

Taking the derivative of Eq. (A.10) w.r.t. b,

$$\frac{\partial b_1}{\partial b} = -\frac{4b\Big(b-1\Big)\Big(2 + b(q-2)\Big)\Big(1 + b(q-1)\Big)}{\Big(1 + b^2(q-1)\Big)^2}, \quad \text{(A.11)}$$

which is evaluated at b to obtain the numeric derivative value. All partial derivatives of the new Boltzmann pair-coupling w.r.t. to the old Boltzmann pair-coupling will be of the same form. Next, the partial derivatives of the coefficients $\partial J(b)/\partial b$, $\partial J(b_1)/\partial b_1$, etc. Recall, the coefficient form,

$$J_l(b) = n_{l-1}^b \log g'(b,q). \quad \text{(A.12)}$$

Similar to the derivatives of b_1, the partial derivatives of J at $b, b_1, b_2, ...$ are all the same derivative of $\log g$ evaluated at the respective point. Recall the dedecorated, renormalized g' as a function of b, q in the absence of an external field,

$$g'(b,q) = \Big(1 + b^2 + b^2(q-2)\Big)^2. \tag{A.13}$$

Take the log, then differentiate w.r.t. to b,

$$\frac{\partial\Big(\log g'(b,q)\Big)}{\partial b} = \frac{4b(q-1)}{1+b^2(q-1)}, \tag{A.14}$$

and then evaluate at numeric point b. The quantity Eq. (A.14) will be the same form for all levels of dedecoration. Finally, the brute force partition function of the q-state Potts model at L_1 and arbitrary renormalized dedecorated coupling is

$$Z_1(b_k) = \sum_s {b_k}^{\Theta(s_1 \neq s_2)}, \tag{A.15}$$

and can be resolved for b_k, q as,

$$Z_1(b_k, q) = q^2 + q(b_k - 1). \tag{A.16}$$

The derivative of the log of Eq. (A.16) for b_k follows easily. All the results Eqs. (A.11), (A.14), and (A.16) that make up Eq. (A.8) can be defined as subroutines so no actual large symbolic derivatives need to be taken during recursion. As long as correct book keeping of which n_l^b we are at in each level is maintained the value for the total energy can be obtained very quickly by these numeric methods.

Now, consider $\partial/\partial b$ of Eq. (A.2) which will lead us to the expression for the heat capacity of the q-state Potts model

$$\begin{aligned}\frac{\partial}{\partial b}\frac{\partial}{\partial b}F_l(b) = \frac{\partial}{\partial b}\frac{\partial}{\partial b}J_l(b) + \\ \left(\frac{\partial}{\partial b}\frac{\partial}{\partial b}b_1(b)\right)\frac{\partial}{\partial b_1}F_{l-1}(b_1) + \\ \frac{\partial}{\partial b}b_1\left(\frac{\partial}{\partial b}\frac{\partial}{\partial b_1}F_{l-1}(b_1)\right).\end{aligned} \tag{A.17}$$

Using chain rule on the last term and the superscript notation for derivatives we write Eq. (A.17) as

$$F_l{}^{(2)}(b) = J_l{}^{(2)}(b) + b_1{}^{(2)}(b) F_{l-1}{}^{(1)}(b_1) + \Big(b_1{}^{(1)}(b)\Big)^2 F_{l-1}{}^{(2)}(b_1). \tag{A.18}$$

Reiterate, distribute, and group together the terms in Eq. (A.18) to get for a finite system in the form $F^{(2)} = F_{\mathrm{I}}^{(2)} + F_{\mathrm{II}}^{(2)} + F_{\mathrm{III}}^{(2)}$,

$$\begin{aligned} F_l{}^{(2)}(b) = \Big[& J_l{}^{(2)}(b) + \Big(b_1{}^{(1)}(b)\Big)^2 J_{l-1}{}^{(2)}(b_1) \\ & + \Big(b_1{}^{(1)}(b)\Big)^2 \Big(b_2{}^{(1)}(b_1)\Big)^2 J_{l-2}{}^{(2)}(b_2) + \ldots \Big]_{\mathrm{I}} \\ & + \Big[b_1{}^{(2)}(b) F_{l-1}{}^{(1)}(b_1) + \Big(b_1{}^{(1)}(b)\Big)^2 b_2{}^{(2)}(b_1) F_{l-2}{}^{(1)}(b_1) \\ & + \Big(b_1{}^{(1)}(b)\Big)^2 \Big(b_2{}^{(1)}(b_1)\Big)^2 b_3{}^{(2)}(b_2) F_{l-3}{}^{(1)}(b_3) + \ldots \Big]_{\mathrm{II}} \\ & + \Big[\Big(b_1{}^{(1)}(b)\Big)^2 \Big(b_2{}^{(1)}(b_1)\Big)^2 \Big(b_3{}^{(1)}(b_2)\Big)^2 \ldots F_1{}^{(2)}(b_k) \Big]_{\mathrm{III}}. \end{aligned} \tag{A.19}$$

The square brackets with subscript I, II, and III denote the grouping of terms. In the first group I,

$$\begin{aligned} F_{\mathrm{I}}^{(2)} = J_l{}^{(2)}(b) + & \Big(b_1{}^{(1)}(b)\Big)^2 J_{l-1}{}^{(2)}(b_1) \\ & + \Big(b_1{}^{(1)}(b)\Big)^2 \Big(b_2{}^{(1)}(b_1)\Big)^2 J_{l-2}{}^{(2)}(b_2) + \ldots \end{aligned} \tag{A.20}$$

The first part of the heat capacity is a sum of the second derivative of the coefficients J with associated squared partials $\partial b_1/\partial b$. The partials have been predefined in the energy analysis of this appendix and to compute the second derivatives of J at the respective Boltzmann point we require the second derivative of Eq. (A.14),

$$\frac{\partial^2 \Big(\log g'(b,q)\Big)}{\partial b^2} = -\frac{4\Big(b^2(q-1)-1\Big)\Big(q-1\Big)}{\Big(1+b^2(q-1)\Big)^2}. \tag{A.21}$$

The second part, II, in Eq. (A.19) is a sum of the total energies at each level of

dedecoration with associated first and second derivatives of $b_1(b,q)$ attached,

$$F_{\rm II}^{(2)} = {b_1}^{(2)}(b){F_{l-1}}^{(1)}(b_1) + \Big({b_1}^{(1)}(b)\Big)^2 {b_2}^{(2)}(b_1){F_{l-2}}^{(1)}(b_1) + \Big({b_1}^{(1)}(b)\Big)^2\Big({b_2}^{(1)}(b_1)\Big)^2 {b_3}^{(2)}(b_2){F_{l-3}}^{(1)}(b_3) + ... \quad \text{(A.22)}$$

The energy, $F_l^{(1)}(b)$, is resolved by our earlier analysis at each level of dedecoration and the squared partials of the form $\partial b_1/\partial b$ is also obtained previously. The one, new piece of Eq. (A.22) is the second derivative of $b_1(b,q)$ w.r.t. internal argument b,

$$\frac{\partial^2 b_1}{\partial b^2} = \frac{-8\Big(b-1\Big)^4\Big(2b-1\Big) + 8bq\Big(b-1\Big)^3\Big(5b-3\Big)}{\Big(1+b^2(q-1)\Big)^4} - \frac{4b^2q^2\Big(b-1\Big)\Big(3+b(8b-13)\Big) + 4b^4q^3\Big(2b-3\Big)}{\Big(1+b^2(q-1)\Big)^4}, \quad \text{(A.23)}$$

These types of derivatives will be the same form for all $\partial^2 b_1/\partial b^2$, $\partial^2 b_2/\partial {b_1}^2, ...$ just evaluated at the respective Boltzmann pair-coupling point of dedecoration. The final piece is part III of Eq. (A.19),

$$F_{\rm III}^{(2)} = \Big({b_1}^{(1)}(b)\Big)^2\Big({b_2}^{(1)}(b_1)\Big)^2\Big({b_3}^{(1)}(b_2)\Big)^2 ... \; {F_1}^{(2)}(b_k). \quad \text{(A.24)}$$

The only piece of Eq. (A.24) not covered previously is the final term, ${F_1}^{(2)}(b_k)$. This term is just the second symbolic derivative of the log of Eq. (A.16) w.r.t. internal coupling parameter and evaluated numerically at b_k which follows easily.

APPENDIX B

: The L_2 Partition Function Polynomial

As an example of how polynomial fitting can be used to compute the partition function consider the L_2 hierarchical lattice without an external field interaction in Boltzmann weight form, $b = e^{\kappa}$,

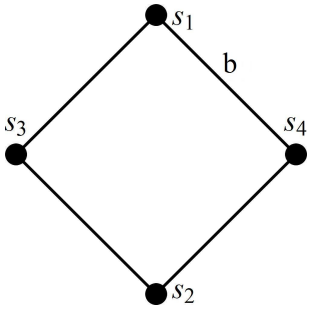

The partition function for this system is defined as

$$Z_2^q(b) = \sum_s b^{(\Theta(s_1 \neq s_3)+\Theta(s_3 \neq s_2)+\Theta(s_2 \neq s_4)+\Theta(s_4 \neq s_1))}. \tag{B.1}$$

We employ brute force counting for increasing q; for $q = 2$,

$$Z_2^{q=2}(b) = 2b^4 + 12b^2 + 2.$$

For $q = 3, 4, 5, 10, 20$,

$$Z_2^{q=3}(b) = 18b^4 + 24b^3 + 36b^2 + 3$$

$$Z_2^{q=4}(b) = 84b^4 + 96b^3 + 72b^2 + 4$$

$$Z_2^{q=5}(b) = 260b^4 + 240b^3 + 120b^2 + 5$$

$$Z_2^{q=10}(b) = 6570b^4 + 2880b^3 + 540b^2 + 10$$

$$Z_2^{q=20}(b) = 130340b^4 + 27360b^3 + 2280b^2 + 20$$

We see a trend on how the resultant partition function changes based on increasing q. The sequence can be mapped to a polynomial that varies as a function of q,

$$Z^q_{2,\text{poly}}(b,q) = \Big(q-1+(q-1)^4\Big)b^4 + \Big(4\big(q-2\big)\big(q-1+(q-1)^2+q\big)\Big)b^3 + \Big(6\big(q-1+(q-1)^2\big)+q\Big)b^2 + q. \quad \text{(B.2)}$$

Results, like Eq. (B.2), can used instead of a brute force calculation of the partition function for a lattice like L_2 at the start of this appendix.

BIBLIOGRAPHY

A.M. Ferrenburg, D. L. and Wong, Y., "Monte Carlo simulations: Hidden errors from 'good' random number generators," *Physical Review*, vol. 69, 3382, 1992.

Ferdinand, A. and Fisher, M., "Bounded and Inhomogenous Ising Models. I. Specific-Heat Anomaly of a Finite Lattice," *Physical Review*, vol. 185, 932, 1969.

Huang, K., *Statistical Mehcanics, 2nd. edn.* Hoboken, New Jersey, United States of America: John Wiley and Sons, INC., 1987.

Ising, E., "Beitrag zur Theorie des Ferromagnetismus," *Zeitschrift fur Physik*, 1925.

Kadanoff, L., "Scaling laws for Ising models near critical temperature," *Physics*, vol. 2, 263, 1966.

Landau, L. D. and Lifshitz, E. M., *Statistical Physics 3rd Edition Part 1.* The Boulevard, Langford Lane, Kidlington, Oxford: Butterworth-Heinemann, 1980.

Newman, M. E. J. and Barkema, G. T., *Monte Carlo Methods in Statistical Physics.* Oxford, New York, United States of America: Oxford University Press, 1999.

Niemeijer, T. and van Leeuwen, J., *Phase transitions and critical phenomena, Voulme 7, Chapter 7.* Waltham, Massachusetts, United States of America: Academic Press, 1972-2001.

Nightingale, M. P., "Private Communication."

Potts, R., "Some Generalized Order-Disorder Transformations," *Mathematical Proceedings*, vol. 48, 1952.

Reichl, L. E., *A Modern Course in Statistical Physics.* Austin, Texas, United States of America: University of Texas Press, 1980.

Schroeder, D. V., *An Introduction to Thermal Physics.* Boston, Massachusetts, United States of America: Addison Wesley Longman, 2000.

TestU01. "Testu01." aug 2009. [Online]. Available: http://www.iro.umontreal.ca/~simardr/testu01/tu01.html

Wikipedia. "Diehard tests." aug 2011. [Online]. Available: http://en.wikipedia.org/wiki/Diehard_tests

Wikipedia. "List of random number generators." apr 2014. [Online]. Available: http://en.wikipedia.org/wiki/List_of_random_number_generators

Wu, F., "The Potts model," *Reviews of Moden Physics*, vol. 54 No. 1, jan 1982.